STATE-OF-THE-ART REVIEW ARTICLE

Intraoperative Transesophageal Echocardiography for Surgical Repair of Mitral Regurgitation

David Andrew Sidebotham, MB ChB, FANZCA, Sara Jane Allen, MB ChB, FANZCA, FCICM, Ivor L. Gerber, MB ChB, MD, FRACP, FACC, and Trevor Fayers, MB ChB, FRACS, FCS(SA), *Auckland, New Zealand; Brisbane, Australia*

Surgical repair of the mitral valve is being increasingly performed to treat severe mitral regurgitation. Transesophageal echocardiography is an essential tool for assessing valvular function and guiding surgical decision making during the perioperative period. A careful and systematic transesophageal echocardiographic examination is necessary to ensure that appropriate information is obtained and that the correct diagnoses are obtained before and after repair. The purpose of this article is to provide a practical guide for perioperative echocardiographers caring for patients undergoing surgical repair of mitral regurgitation. A guide to performing a systematic transesophageal echocardiographic examination of the mitral valve is provided, along with an approach to prerepair and postrepair assessment. Additionally, the anatomy and function of normal and regurgitant mitral valves are reviewed. (J Am Soc Echocardiogr 2014;27:345-66.)

Keywords: Transesophageal echocardiography, Mitral valve repair, TEE, Intraoperative, Cardiac surgery

In suitable patients, surgical repair is an excellent treatment option for severe mitral regurgitation (MR). The procedure is associated with low mortality and is highly durable. Among 58,370 unselected patients from the Society of Thoracic Surgeons Adult Cardiac Surgery database undergoing isolated mitral valve (MV) surgery in the United States between January 2000 and December 2007, operative mortality was 1.4% for valve repair compared with 3.8% for valve replacement.[1] During the study period, the rate of valve repair increased from 51% to 69%. Among a cohort of 14,604 older patients (aged >65 years) undergoing mitral repair, operative mortality was 2.59%, the 10-year reoperation rate was 6.2%, and 10-year survival was 57.4%, equivalent to the matched US population.[2] Although there have been few randomized trials comparing MV repair with replacement, a meta-analysis in 2007 of nonrandomized series demonstrated reduced early mortality and lower rates of thromboembolism for repair compared with replacement.[3] In addition to reduced early mortality for patients with degenerative MV disease (odds ratio, 1.93; 95% confidence interval, 1.08–3.44), mortality was also reduced in patients with functional MR (FMR) (odds ratio, 2.01; 95% confidence interval, 1.19–3.40) and in mixed patient populations (odds ratio, 2.39; 95% confidence interval, 1.76–3.26). However, these data are nonrandomized and subject to selection bias. Older and sicker patients, and those with less favorable valves, are more likely to undergo MV replacement. Notwithstanding the lack of randomized data, for patients with suitable valves, surgical repair is now the preferred option for treating severe MR.

Transesophageal echocardiography (TEE) affords high-quality, real-time assessment of MV structure and function and is uniquely suited to intraoperative use. Consequently, TEE is an essential tool during MV repair surgery.[4,5] Before repair, TEE is used to determine the mechanism, extent, and severity of MR. After repair, TEE is used to evaluate the severity of any residual regurgitation and to diagnose other complications, such as systolic anterior motion (SAM) and mitral stenosis. However, to obtain appropriate information to guide surgical decision making, perioperative echocardiographers must understand the etiology and mechanisms of MR, have an appreciation of surgical techniques, and, most important, be able to perform a comprehensive assessment of MV structure and function in the operating room environment. The primary objective of this review article is to provide an up-to-date, practical guide to perioperative transesophageal echocardiographic assessment of patients undergoing MV repair surgery.

NORMAL ANATOMY AND FUNCTION OF THE MITRAL VALVE

The MV is best conceptualized as a valve complex, comprising an annulus, leaflets, chordae, papillary muscles, and left ventricular muscle. Normal functioning of the MV requires the coordinated activity of all components of the valve complex.

Annulus

The mitral annulus is a fibrofatty ring that approximates a hyperbolic paraboloid, a geometric shape similar to a riding saddle.[6] The annulus has two axes, a shorter and "higher" (more basal) anteroposterior (AP) axis and a longer and "lower" (more apical) commissural axis (Figure 1). The

From the Department of Anesthesia, The Cardiovascular Intensive Care Unit (D.A.S., S.J.A.) and Green Lane Cardiovascular Service (I.L.G.), Auckland City Hospital, Auckland, New Zealand; and Department of Cardiac Surgical Services, Holy Spirit Northside Hospital and The Prince Charles Hospital, Brisbane, Australia (T.F.).

Correspondence: David Andrew Sidebotham, MB ChB, FANZCA, Auckland City Hospital, Cardiothoracic and Vascular Intensive Care Unit, Auckland, New Zealand (E-mail: *dsidebotham@adhb.govt.nz*).

0894-7317/$36.00

http://dx.doi.org/10.1016/j.echo.2014.01.005

Abbreviations

AP = Anteroposterior

CPB = Cardiopulmonary bypass

EROA = Effective regurgitant orifice area

FED = Fibroelastic deficiency

FMR = Functional mitral regurgitation

LVEF = Left ventricular ejection fraction

LVOT = Left ventricular outflow tract

MR = Mitral regurgitation

MV = Mitral valve

NL = Nyquist limit

PISA = Proximal isovelocity surface area

PVR = Pulmonary vascular resistance

SAM = Systolic anterior motion

TEE = Transesophageal echocardiography

3D = Three-dimensional

TR = Tricuspid regurgitation

2D = Two-dimensional

VCA = Vena contracta area

VCW = Vena contracta width

anterior pole of the AP axis corresponds to the "riding horn" of the saddle and the commissural axis to the "seat" of the saddle. Anteriorly, the mitral annulus is thickened and fixed to the aortic annulus, a region termed the intervalvular fibrosa. The saddle shape of the mitral annulus acts to reduce tension on the leaflets, particularly the middle scallop of the posterior leaflet.[7,8] Annular height is normalized to annular size by the ratio of height to commissural length at end-systole and is normally about 15%.[8] Leaflet tension increases dramatically when this ratio falls below 10% (i.e., when the annulus becomes planar [decreased height] or dilated [increased commissural length]).

Ventricular contraction results in important conformational changes in the mitral annulus (Figure 1).[9-11] In early systole, left ventricular contraction causes a sphincter-like decrease in posterior annular area. The annulus shortens along the AP axis, and overall annular area is reduced by approximately 25%. Ventricular contraction also causes systolic folding of the anterior annulus, leading to a deepening of the saddle. The AP diameter returns to normal in midsystole, but increased annular height is maintained throughout systole. Annular folding and sphincteric contraction reduce leaflet tension and aid leaflet apposition, particularly in early systole when ventricular pressure is low.[8-10]

Leaflets

The MV has an anterior and a posterior leaflet (Figure 2). The anterior leaflet is oriented slightly medially (rightward) and the posterior leaflet slightly laterally (leftward). The leaflet edges meet at two commissures, termed anterolateral and posteromedial. The anterior leaflet is thicker, has a shorter annular attachment, and has a longer base-to-tip length than the posterior leaflet. In most people, the posterior leaflet is composed of three distinct scallops, which are not present on the anterior leaflet. Pleating of the scallops aids closure of the C-shaped posterior leaflet. By contrast, the anterior leaflet does not alter its circumferential length during systole, and therefore no pleating mechanism is required. Leaflet segments are usually named using the system popularized by Carpentier (Figure 2).[12] This nomenclature is useful for defining the location of leaflet pathology and for describing the relationship of the annulus to adjacent cardiac structures. The edges of the leaflets meet at a curved coaptation line that runs roughly along the commissural axis. There is normally approximately 10 mm of leaflet overlap (coaptation height) at end-systole.

Papillary Muscles, Chordae, and Left Ventricle

Two papillary muscles, the anterolateral and the posteromedial, support the mitral leaflets. The papillary muscles run parallel with the long axis of the left ventricle, aligned with the commissures. Systolic contraction of the papillary muscles offsets the base-to-apical shortening of the left ventricle, which would otherwise cause leaflet prolapse. The larger anterolateral muscle typically arises from the mid anterolateral wall of the left ventricle and supports the ipsilateral half of both leaflets: A1/P1 and the anterolateral part of A2/P2. The smaller posteromedial muscle typically arises from the mid inferior wall of the left ventricle and supports the ipsilateral part of both leaflets: A3/P3 and the posteromedial part of A2/P2. Branches of the left anterior descending and circumflex coronary arteries supply the anterolateral muscle, whereas the posteromedial muscle is supplied entirely by branches of the right coronary artery and is therefore more vulnerable to rupture after myocardial infarction.

The papillary muscles attach to the leaflets via chordae tendineae. Primary chords attach to the free edges of the leaflets, and secondary chords attach to the undersurface of the leaflets. Primary chords support the free edges of the leaflets during systole. Rupture of primary chords causes acute MR. Secondary chords help maintain left ventricular geometry, particularly the two thicker strut chords, which attach to the undersurface of the anterior leaflet.[6]

ETIOLOGY OF MITRAL REGURGITATION

In developed countries, degenerative disease and FMR are the two most common indications for surgical treatment of MR, accounting for approximately 70% and 20% of cases, respectively.[13] Rheumatic heart disease is relatively uncommon in developed nations but remains the most frequent cause of valvular heart disease in developing countries. Other important causes of MR include endocarditis, clefts, and papillary muscle rupture.

Degenerative MR

Degenerative MV disease encompasses a range of pathology, including chordal stretching or rupture, leaflet thickening and redundancy, annular dilatation, and calcification of the leaflets and chordae. Leaflet and chordal thickening is due to proliferation of cellular and connective tissue elements, particularly the accumulation of glycosaminoglycans in the extracellular matrix,[14,15] a process termed myxomatous change.

Two forms of degenerative disease are recognized: fibroelastic deficiency (FED) and Barlow disease.[16,17] With FED, there is chordal elongation or rupture resulting in prolapse or flail of an isolated segment, most commonly P2. The affected segment may be morphologically normal or demonstrate myxomatous change. Annular dimensions are only mildly increased. Patients with FED are typically older (aged >60 years) and have short clinical histories consistent with the abrupt onset of MR due to chordal rupture. Barlow disease is characterized by widespread myxomatous change involving multiple leaflet segments and the subvalvular apparatus. Patients are often younger (aged <60 years) and have long-standing MR. Although FED and Barlow disease are separate clinical entities, they represent two ends of a disease spectrum. Barlow disease is associated with mitral annular disjunction, in which there is wide separation (5–15 mm) between the left ventricular wall and the atrial wall–MV junction posteriorly, resulting in hypermobility of the posterior annulus.[18] Degenerative MV disease usually occurs in isolation but

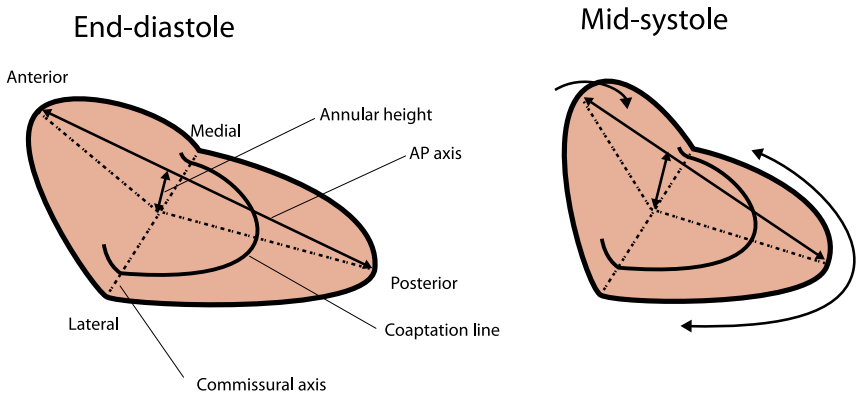

Figure 1 Schematic demonstrating the 3D shape and motion of the mitral annulus. During systole, contraction along the AP axis results in reduced annular area, and folding along the commissural axis results in increased annular height. See text for details.

is also associated with systemic connective tissues disorders such as Marfan and Ehlers-Danlos syndromes.

Quantitative three-dimensional (3D) echocardiography demonstrates important abnormalities in valvular dimensions and motion in patients with degenerative MV disease.[10,19,20] Values for annular area, leaflet area, AP diameter, commissural diameter, and prolapse height are all increased compared with normal, being greater for Barlow disease than FED.[10,19] The ratio of commissural diameter to AP diameter is reduced with Barlow disease compared with FED, reflecting the more circular shape of the annulus in Barlow disease.[19] Annular dynamics are also abnormal. During systole, shortening along the AP axis occurs normally, but there is marked pathologic expansion along the commissural axis in late systole, leading to a diminished reduction in annular area, which exacerbates MR.[10] Annular folding is also reduced, resulting in a more planar annulus, which also contributes to MR.[10]

Successful repair of degenerative MV disease is possible in the majority of patients, particularly when disease is limited to the posterior leaflet. Anterior and bileaflet repairs are more challenging and are associated with a lower rate of success and a higher need for reoperation.[21,22] However, success for all types of repairs is increasing. In recent series, success rates approaching 100% have been reported for isolated posterior leaflet repairs.[23,24] For complex anterior and bileaflet repairs, success rates of >90% have been reported at high-volume centers.[25,26] These figures are unlikely to be achieved in nonspecialist units.

FMR

FMR is MR that occurs in the presence of structurally normal mitral leaflets. FMR may be ischemic or nonischemic, the latter due primarily to dilated cardiomyopathy. The main mechanism of FMR is leaflet tethering due to ventricular dilatation.[27,28] Left ventricular remodeling causes lateral and/or apical displacement of the papillary muscles, resulting in leaflet tethering in systole. However, the relationship between ventricular dilatation and MR is complex. FMR is more common after inferior or posterior myocardial infarction than anterior infarction, despite greater ventricular dilatation with the latter (Figure 3).[29-31] Inferior or posterior infarction causes more displacement of the posteromedial papillary muscle than occurs to the anterolateral papillary muscle after anterior infarction.[29] There are several reasons for the reduced impact of anterior infarction on mitral geometry[31]: the annulus is better supported anteriorly by the intervalvular fibrosa, the ventricular septum helps prevent lateral displacement of the anterolateral papillary muscle, and anterior infarctions tend to be more apical, with relative sparing of the basal left ventricular wall.

Left ventricular systolic dysfunction and annular dilatation contribute to FMR but are not primary etiologic mechanisms. In clinical studies, there is an inconsistent relationship between left ventricular ejection fraction (LVEF) and the severity of FMR.[32,33] Thus, it is not unusual for patients with severe left ventricular dysfunction to have minimal FMR and vice versa. Annular dilatation, particularly along the AP axis, is a consistent finding but is less marked than with degenerative MR.[10,20,34] Annular height is variable, but in general, the annulus is more planar than normal.[10,20,34] During systole, there is reduced contraction along the AP axis and a minimal increase in annular height.[20]

Isolated annular dilatation, in the absence of ventricular remodeling, is an uncommon cause of FMR but can occur because of atrial dilatation secondary to atrial fibrillation.[35]

The durability of MV repair for FMR is less than for degenerative disease, with recurrence rates for moderate or severe MR of 20% to 30% typical.[36-38] Recurrence is more likely when annular dilatation is severe and there is marked leaflet tethering (see below).[36,39] In a recently published randomized trial, no difference in survival was observed between repair or replacement for severe FMR, but recurrence of moderate or severe regurgitation was 32.6% for repair versus 2.3% for replacement at 12-month follow-up.[38] However, the trial was not powered to detect a mortality difference, and given the randomized design, some patients at high risk for recurrence would have undergone valve repair.

Rheumatic Disease, Endocarditis, Clefts, and Papillary Muscle Rupture

Rheumatic MR is characterized by leaflet thickening and retraction, chordal shortening, and commissural fusion. Leaflet motion is restricted in both systole and diastole, and the leaflet tips have a characteristic rolled-edge appearance. Calcification may be present in the annulus, leaflets, and subvalvular apparatus. Valve repair for rheumatic MR is challenging and associated with a high failure rate.[40,41] In most circumstances, valve replacement is the preferred treatment.

Endocarditis can occur on normal valves but is more common on diseased valves. MR arises because of leaflet perforation, destruction, or deformity. Leaflet perforation commonly occurs at the site of attachment of vegetations. Endocarditis can also cause aneurysm or abscess formation in the valve and surrounding tissues, which may perforate causing MR.[42-44] If leaflet destruction is not severe, MV repair is feasible in most patients.[45]

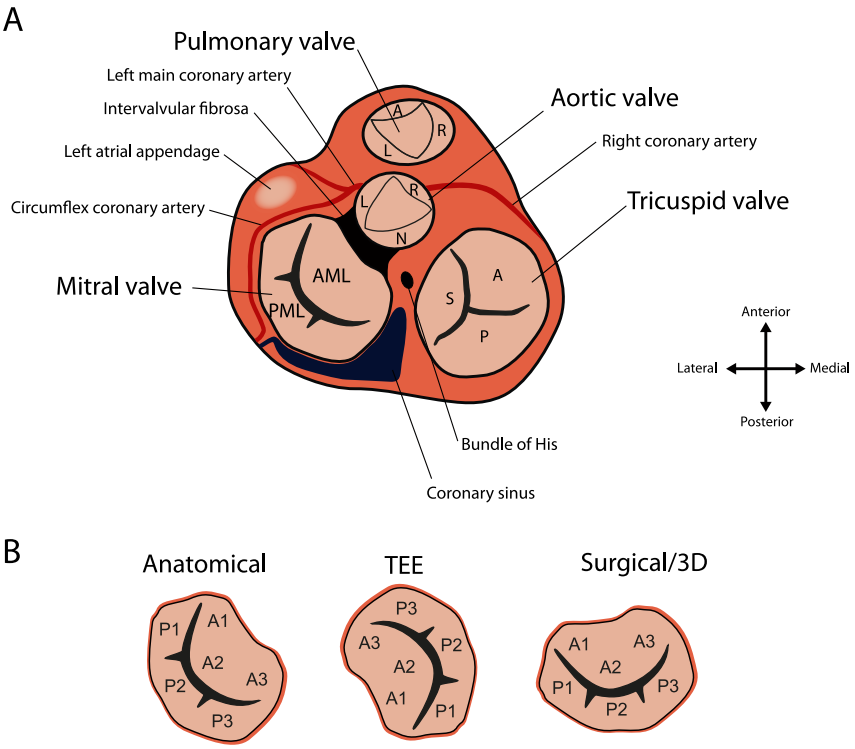

Figure 2 Schematic demonstrating the anatomic relationships, leaflet nomenclature, and orientation of the MV. **(A)** The four heart valves are shown in an anatomic orientation, from the base (atrial aspect) of the heart. The relationship of the MV to the aortic valve, left atrial appendage, circumflex coronary artery, coronary sinus, and bundle of His are demonstrated. **(B)** Carpentier nomenclature for the mitral segments with the MV shown in three different orientations. The anterolateral, middle, and posteromedial scallops of the posterior leaflet are termed P1, P2, and P3, respectively, and the adjacent segments of the anterior leaflet are termed A1, A2, and A3. In the anatomic view, the valve is displayed from the base of the heart with the left atrium cut away. The patient's left and right correspond to the observer's left and right. The AP axis of the valve does not lie in a true AP axis but is rotated slightly clockwise with the anterior leaflet orientated slightly medially (*rightward*) and the posterior leaflet orientated slightly laterally (*leftward*). The A1/P1 segments are anterior and lateral (adjacent to the anterolateral commissure), and the A3/P3 segments are posterior and medial (adjacent to the posteromedial commissure). In the transesophageal echocardiographic view, the valve is rotated clockwise 180° from the anatomic view. This is the orientation of the MV that is seen in the transgastric basal short-axis view. The surgical view is the view the surgeon has standing on the patient's right looking through a left atrial incision. This is also the standard orientation to display 3D data sets. In the surgical or 3D view, the AP axis of the valve does appear in a true AP orientation. A1/P1 is on the left, adjacent to the left atrial appendage, and A3/P3 is on the right, adjacent to the coronary sinus. The aortic valve lies above the MV, adjacent to A2. *A*, Anterior leaflet of pulmonary and tricuspid valves; *AML*, Anterior mitral leaflet; *PML*, posterior mitral leaflet; *L*, left leaflet of pulmonary and aortic valves; *N*, noncoronary leaflet of the aortic valve; *P*, posterior leaflet of tricuspid valve; *R*, right leaflets of pulmonary and aortic valves; *S*, septal leaflet of tricuspid valve.

Mitral clefts are typically congenital in origin. Anterior clefts are more common than posterior clefts and usually occur in association with other congenital heart disease, particularly endocardial cushion defects such as inlet ventricular septal defect or primum atrial septal defect.[46] Clefts of the posterior leaflet are very uncommon and are not associated with other congenital heart disease.[47] Clefts that present in adulthood are strongly associated with degenerative MV disease, at least for the posterior leaflet.[47] Degenerative change may reflect regurgitation-induced mechanical injury.[48] The great majority of mitral clefts can be successfully repaired.[47]

Most cases of papillary muscle rupture are due to myocardial infarction, but rupture occasionally occurs after chest trauma. Rupture of the posteromedial muscle is associated with inferior myocardial infarction and occurs approximately 10 times more commonly than rupture of the anterolateral muscle, reflecting the single-vessel blood supply to the former.[49,50] MV replacement is usually required.

TRANSESOPHAGEAL ECHOCARDIOGRAPHIC ASSESSMENT OF THE MITRAL VALVE

Patients undergoing MV repair should undergo a systematic transesophageal echocardiographic examination according to published guidelines.[51] In addition, the MV apparatus should be further examined using a combination of two-dimensional (2D) and 3D imaging (Figure 4). Two-dimensional and 3D imaging are complementary modalities, each with its own strengths and limitations. In general, qualitative 3D imaging is more suitable to the operating room environment than quantitative analysis. Qualitative 3D imaging is more accurate than standard 2D imaging in localizing leaflet pathology,[52] whereas 2D imaging is superior to qualitative 3D imaging for making measurements and for rapidly quantifying severity. In standard 2D and 3D views, it is important to adjust the depth or zoom function to focus on the mitral apparatus and to examine the valve with and without color Doppler.

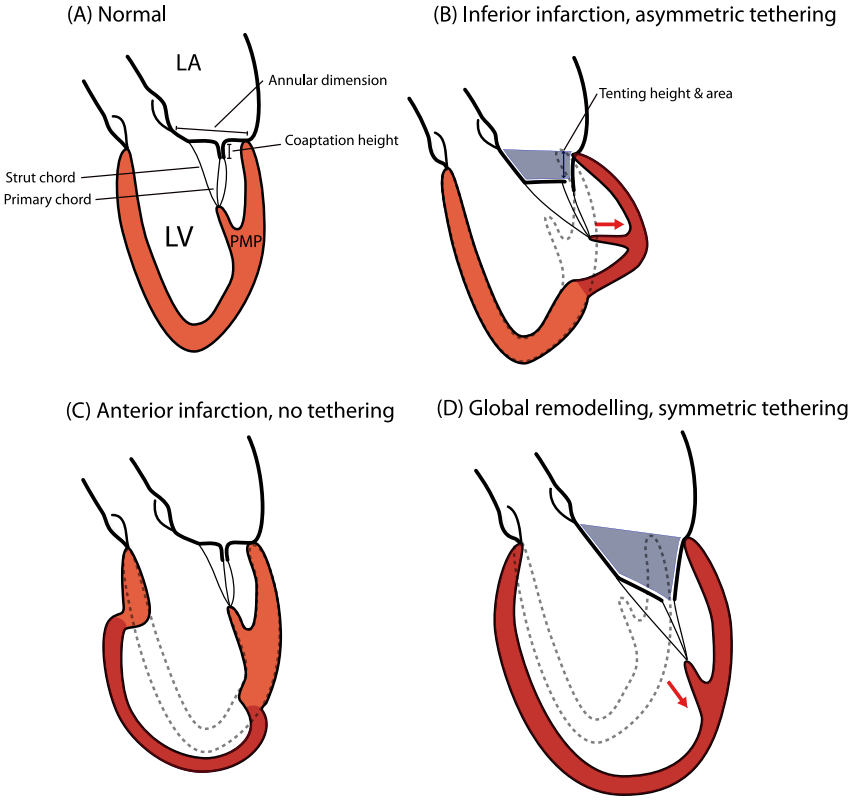

Figure 3 Leaflet tethering patterns and FMR. **(A)** Normal appearances of the mitral leaflets at end-systole. The plane of coaptation is at the level of the annular plane, and there is significant leaflet overlap (coaptation height). **(B)** Effect of inferior or posterior myocardial infarction. Localized remodeling (*shaded red*) causes lateral displacement (indicated by the *directional arrow*) of the posteromedial papillary muscle (PMP), leading to leaflet tethering, particularly of the posterior leaflet, and anterior leaflet override. If present, the jet of MR is posteriorly directed. Tenting area is the area bounded by the mitral leaflets and the annular plane and is normally 0 mm^2. Tenting height is the distance from the leaflet tips to the annular plane, and is normally < 5 mm. **(C)** Effect of anterior myocardial infarction. Remodeling (*shaded red*) after anterior infarction typically involves more myocardium than inferior infarction but causes less leaflet tethering. See text for details. **(D)** Symmetric leaflet tethering due to apical and lateral displacement (indicated by the *red directional arrow*) of both papillary muscles. The coaptation point is displaced well into the left ventricle (LV), resulting in a marked increase in tenting height. There may be a central jet of MR. Symmetric tethering is associated with dilated cardiomyopathy and global remodeling after anterior myocardial infarction. If present, the jet of MR is typically central. *LA*, Left atrium.

Orientation of the MV can be confusing; the three commonly used orientations are shown in Figure 2.

Echocardiographic-Anatomic Correlations

Various "roadmaps" have been published describing the anatomic-echocardiographic relationships for the standard midesophageal views.[53-56] However, differences exist regarding which leaflet segments are visualized in each view, particularly with respect to the four-chamber view, which has variously described as visualizing A2/P2,[53] A2/A1/P2,[56] and A2/A3/P2/P3.[54] Furthermore, in a recent study by Mahmood *et al.*,[57] in which experienced echocardiographers were shown a video sequence of various midesophageal views, the correct mitral segments were identified in only 30.4% of cases. Correct identification of A2 and P2 occurred 69.4% of the time in the long-axis view and 50% of the time in the four-chamber view. A1 and P1 were correctly identified 13.89% of the time in the long-axis view and 47.2% of the time in the four-chamber view, while correct identification of A3 and P3 occurred in only 5.6% of cases in both views. In the commissural view, the correct segments were identified 92% of the time. The reasons for the low success rate include individual variability in cardiac shape and position and the lack of anatomic references in the four-chamber and long-axis views (Figure 5). By contrast, qualitative 3D imaging in the en face view (Figure 6) allows all mitral segments to be identified accurately.[52,58,59]

Midesophageal Views

In the four-chamber view (Figure 4A) the anterior leaflet (usually A2) is on the left, and the posterior leaflet (usually P2) is on the right of the image. The scan plane typically cuts the coaptation line slightly obliquely. In a high or mid probe position, the anterior leaflet appears relatively longer, whereas when the probe is deep, the posterior leaflet appears relatively longer. Oblique imaging is confirmed by visualizing the posteromedial papillary muscle on the right of the image. Withdrawing or anteflexing the probe sweeps the image plane toward the anterolateral commissure (A1/P1) and displays the left ventricular outflow tract (LVOT). Advancing or retroflexing the probe sweeps the image plane toward the posteromedial commissure (A3/P3).

In the commissural view (Figure 4B), the MV appears trileaflet, with P1 on the right, A2 in the center, and P3 on the left. The anterolateral papillary muscle may be visible on the right and the posteromedial papillary on the left of the image. The image plane runs parallel to

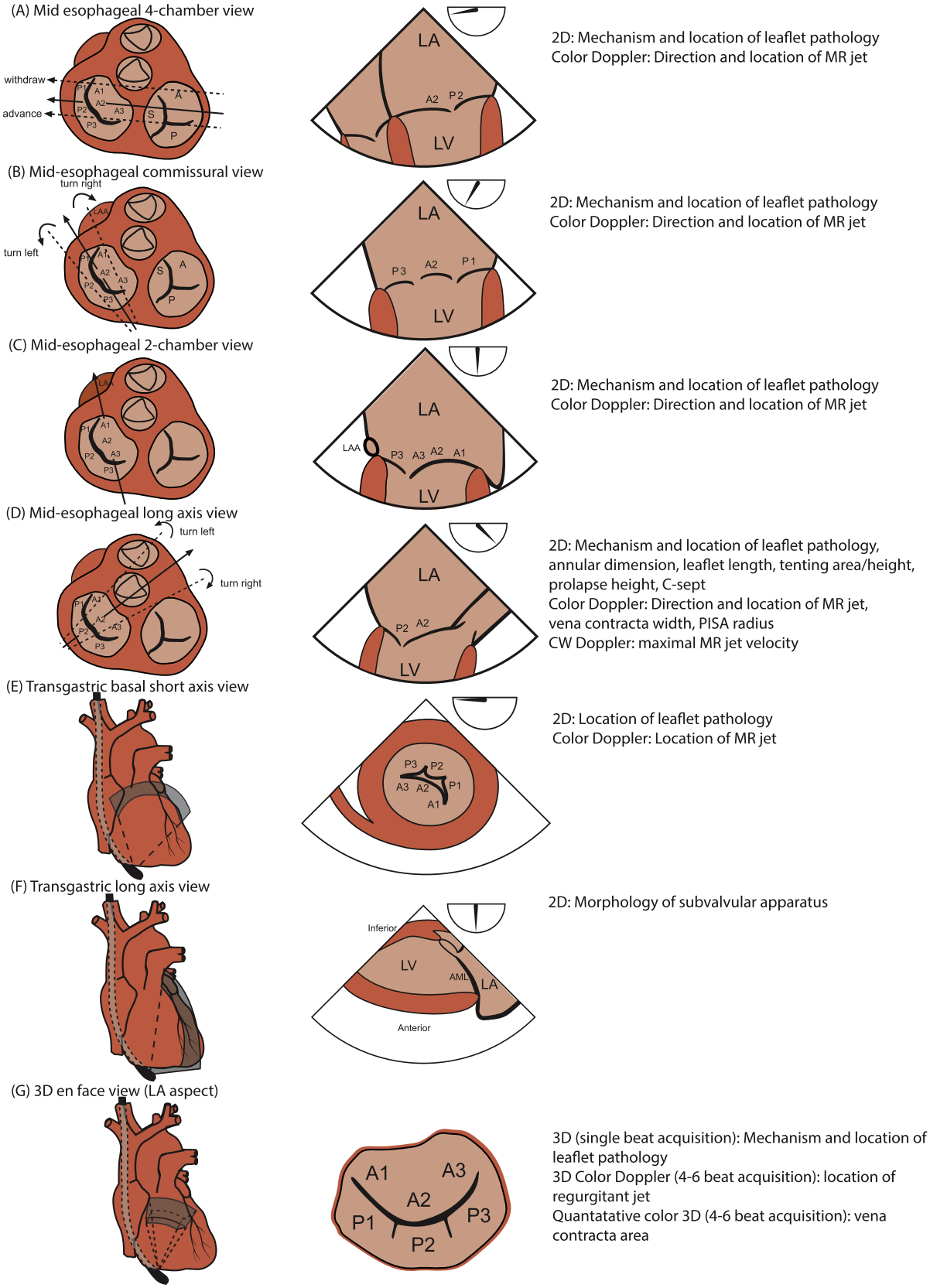

Figure 4 Standard transesophageal echocardiographic views of the MV with suggested examinations in each view. *AML*, Anterior mitral leaflet; *CW*, continuous wave; *LA*, left atrium; *LAA*, left atrial appendage; *LV*, left ventricle. Modified from Sidebotham D, Legget ME, Sutton T. The mitral valve. In: Sidebotham D, Merry AF, Legget ME, Edwards ML. Practical perioperative transesophageal echocardiography. 2nd ed. Philadelphia: Elsevier; 2011:135-162.

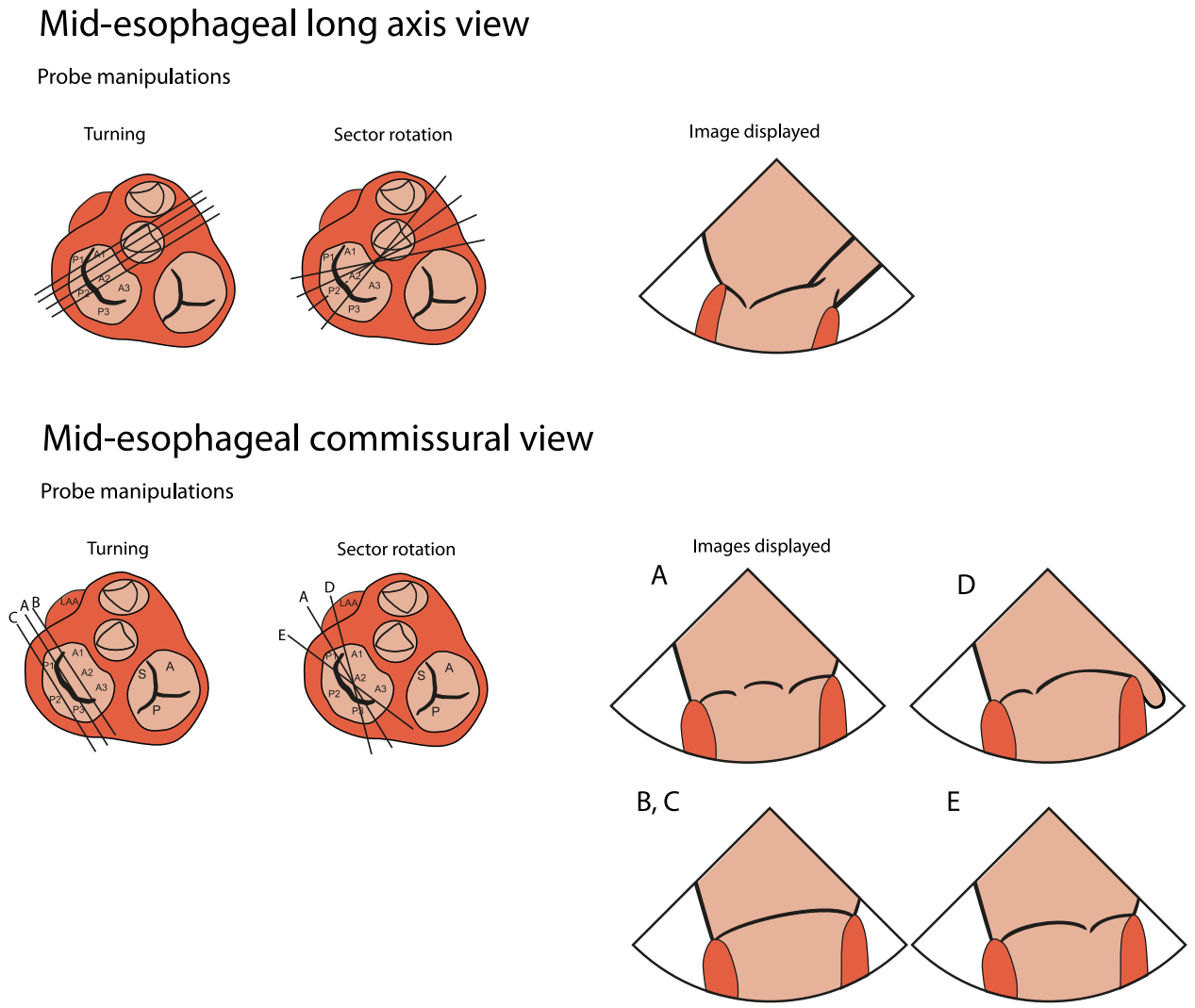

Figure 5 Ambiguity with standard midesophageal imaging. Midesophageal long-axis and commissural views are demonstrated. For the long-axis view, turning the probe or adjusting the sector rotation from the standard position results in minimal change in the displayed image but important changes in which mitral segments are being interrogated. In contrast, for the commissural view, turning the probe or adjusting the sector rotation from the standard position results in changes to the displayed images coincident with changes in the displayed mitral segments. Labels **A** to **E** on the left-hand images correspond to labels **A** to **E** on the displayed images on the right. *LAA*, Left atrial appendage.

the axis of the curved coaptation line, which can result in a broad or double jet of MR when the regurgitant orifice is elliptical (Figure 7). The commissural view passes through the "low," "long" axis of the MV, yielding higher values for annular dimension and prolapse height compared with the long-axis view. A flail or prolapsing P2 segment may appear to rise above A2 in the center of the valve during systole (the cobra sign; Figure 8). In the two-chamber view (Figure 4C), the three segments of the anterior leaflet (A3/A2/A1) are to the right, and P3 is to the left of the image. The coaptation line is cut at A3/P3. The left atrial appendage is on the right, and the coronary sinus is on the left.

In a true long-axis view (Figure 4D), the mitral and aortic valves are both visualized, but neither papillary muscle is seen. When correctly obtained, the long-axis view cuts the coaptation line perpendicularly through A2/P2, along the "high," "short" axis of the valve. Turning the probe to the left (counterclockwise) sweeps the scan plane toward the anterolateral commissure (A1/P1) and, eventually, the left atrial appendage. Turning the probe to the right (clockwise) sweeps the scan plane toward the posteromedial commissure (A3/P3) and, eventually, the right atrium.

Transgastric Views

The basal short-axis view (Figure 4E) provides an en face view of the MV, potentially displaying all mitral segments. With color Doppler imaging, it is sometimes possible to identify the segments (e.g., A1/P1), but not necessarily the leaflet, involved. However, to visualize the regurgitant jet, the image plane must be sufficiently basal (i.e., at or above the annular plane in systole), which is frequently not possible. The two-chamber view (Figure 4F) is useful for visualizing the subvalvular apparatus.

Three-Dimensional Imaging

The recommended orientation for displaying the MV with 3D imaging is en face from the left atrial side in the surgical orientation (Figure 6).[60] This view facilitates unambiguous communication

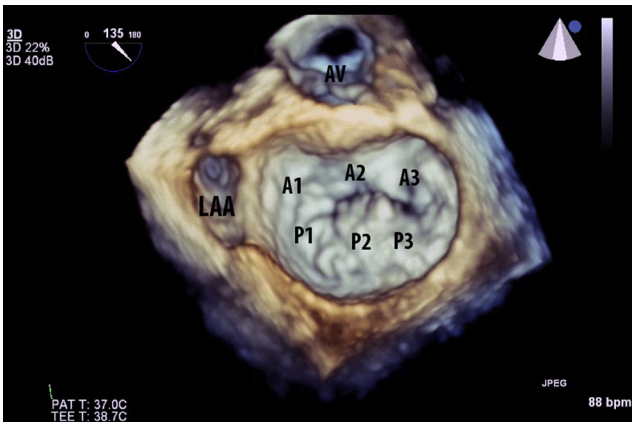

Figure 6 En face view of the MV on 3D TEE. The MV is displayed in the surgical orientation from the left atrial aspect. The left atrial appendage (LAA) and aortic valve (AV) are included in the image to help orient the valve.

between the echocardiographer and surgeon and allows all mitral segments to be accurately identified. The aortic valve and left atrial appendage should be included in the data set, as this helps when orienting the image.

Three-dimensional data sets may be acquired in a single heartbeat (real time) or over several heartbeats. With multiple-beat acquisition, narrow volumes of data are acquired each heartbeat and electronically stitched together. Real-time acquisition is less affected by electrocautery and movement but has lower temporal and spatial resolution than multiple-beat acquisition. Disconnecting the patient from the ventilator and pausing diathermy can minimize movement and electrocautery artifacts. Single-beat acquisition is usually satisfactory for standard 3D imaging, but to achieve adequate resolution, multiple-beat acquisition, over four to six heartbeats, is necessary for color 3D imaging. Zoomed mode is preferred over full-volume mode, as the data set can be limited to the MV, further improving resolution.

EXAMINATION BEFORE CARDIOPULMONARY BYPASS

The goals of the transesophageal echocardiographic examination before cardiopulmonary bypass (CPB) are to assess the mechanism, location, and etiology of the regurgitation; to grade severity; and to identify associated pathology such as ventricular dysfunction, pulmonary hypertension, and tricuspid regurgitation (TR). For minimally invasive MV surgery, TEE is also used for assessing the position of cannulae used for CPB.[61,62]

Assessing Valvular Morphology

Annulus. Degenerative and FMR are associated with annular dilatation. The annulus should be measured at end-systole in the midesophageal long-axis view with the calipers placed at the base of the aortic valve and the hinge point of the posterior mitral leaflet.[63] Using the base of the aortic valve, rather than the hinge point of the anterior leaflet, includes the intervalvular fibrosa and therefore overestimates the true annular dimension by approximately 5 mm. The aortic valve is chosen because the hinge point of the anterior leaflet is often difficult to assess in patients with MV disease.[63] Using this dimension, the upper limit of normal for the mitral annulus is 35 mm, with values $>$ 40 mm considered to indicate severe dilatation. If not diseased, the length of the anterior mitral leaflet provides a useful guide to the appropriate annuloplasty size. The anterior mitral leaflet length is measured from the base of the aorta to the leaflet tip in the midesophageal long-axis view in late diastole, when the leaflet is straight.

The finding of mitral annular calcification or mitral annular disjunction should be discussed with the surgeon, as these findings may complicate the surgery or, in the case of mitral annular disjunction, necessitate the reattachment of the annulus to the ventricular endocardium as part of the repair procedure.[18]

Leaflets. MV pathology may be classified on the basis of leaflet motion (Figure 9).[64] Excessive leaflet motion (type 2) is typically due to degenerative disease and involves leaflet flail, prolapse, or both (Figure 10). Prolapse occurs because of excessive leaflet tissue and/or chordal lengthening. During systole, the body of the leaflet domes above annular plane, but the leaflet tip is directed toward the left ventricle. Less severe prolapse, in which the leaflet tip remains in the ventricle at end-systole, is termed "billowing." Prolapse height should be assessed in the midesophageal long-axis view (i.e., the "high" axis), to avoid overdiagnosis. Leaflet flail occurs because of chordal (or, occasionally, papillary muscle) rupture. The leaflet tip is directed toward the left atrium, and ruptured chordae may be seen flicking in the left atrium in late systole. Isolated prolapse and flail cause eccentric regurgitation, with the jet directed away from the affected side. Ruptured chordae arising from the anterolateral (P1/A1) and posteromedial (P3/A3) segments can flick into the central part of the valve (P2/A2) in late systole, which, with 2D imaging, can give the false impression of P2/A2 flail. However, with 3D imaging, the origin of the chordae is usually readily apparent. Color 3D imaging helps localize the origin of regurgitant jets, which may not directly match the leaflet pathology seen with 2D or 3D imaging (Figure 11).

Restricted leaflet motion is associated with rheumatic (type 3a) and functional (types 3b and 3c) MR. Restriction due to FMR may be symmetric or asymmetric (Figure 3). Asymmetric leaflet tethering (type 3c) occurs because of lateral displacement of the posteromedial papillary muscle and is associated with inferior or posterior myocardial infarction. Posterior leaflet tethering, particularly of P3, tends to be more marked than anterior leaflet tethering.[65,66] The anterior leaflet overrides the posterior leaflet, and the plane of coaptation lies below the annular plane. The regurgitant jet is posteriorly directed (i.e., toward the affected side). Symmetric leaflet tethering (type 3b) occurs because of apical and lateral displacement of both papillary muscles and is associated with dilated cardiomyopathy or a large anterior myocardial infarction.[66,67] There is bileaflet tethering and a central jet of regurgitation.

Measurement of tenting area and annular dimension (Figure 3) helps predict the likelihood of achieving a successful repair. In one study, tenting area $\geq$ 160 mm^2 and annular dimension $\geq$ 37 mm (midesophageal long-axis view) were strongly predictive of surgical failure.[36]

Leaflet clefts (Figure 12) or perforations (Figure 13) may be visualized directly or suggested by a color jet that is displaced from the coaptation line. A congenital anterior leaflet cleft is associated with a posteriorly directed regurgitant jet. Three-dimensional imaging is useful for visualizing clefts and perforations that are not apparent with 2D imaging. Three-dimensional imaging from the left ventricular aspect may help visualize perforations that are hidden by vegetations on the left atrial surface. In patients with severe degenerative disease, in-folding of bulky leaflet tissue can result in color jets seemingly occurring through the body of the leaflet, creating the false impression of a cleft.

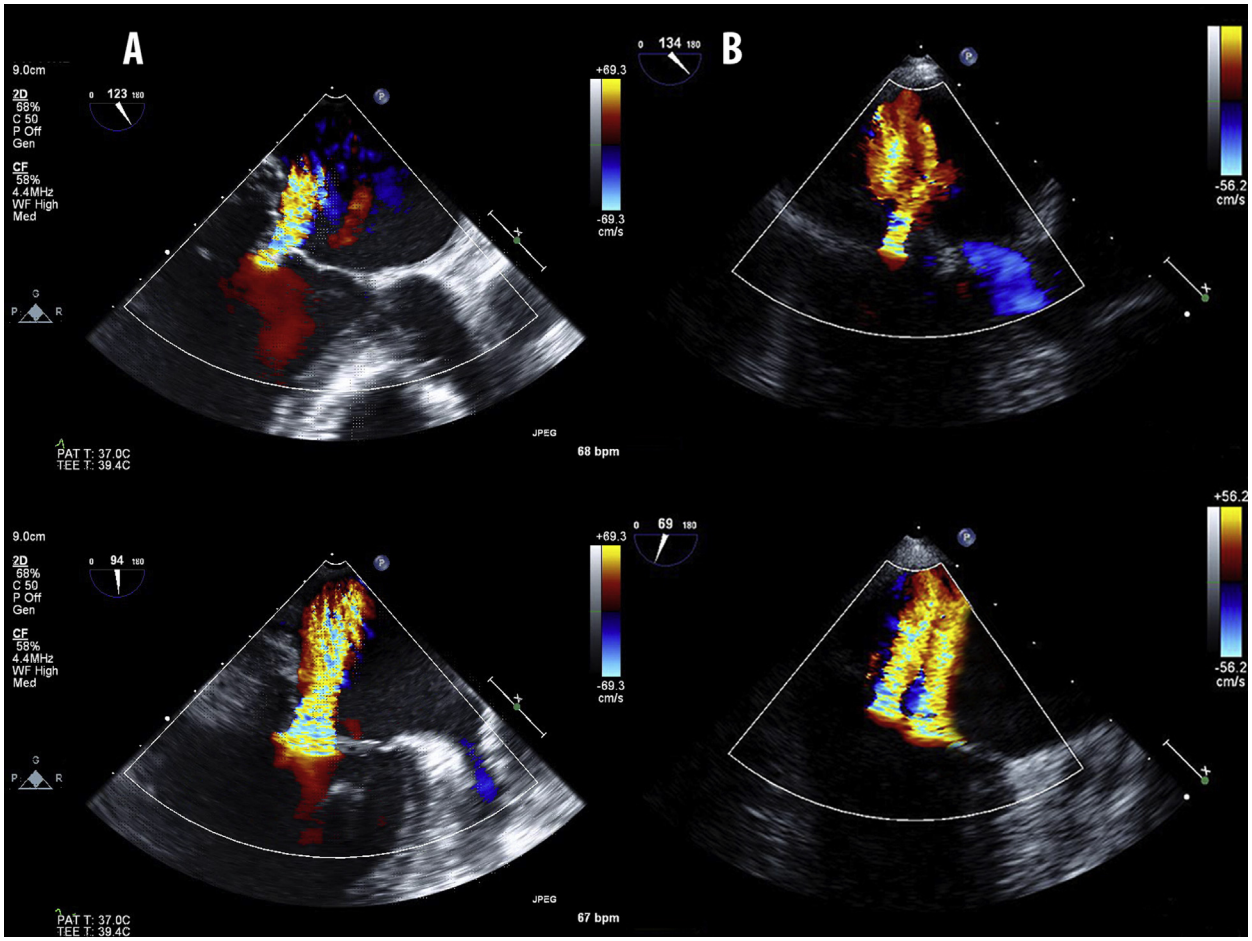

Figure 7 The effect of the image plane on the size and shape of the mitral regurgitant jet. **(A)** In the top frame, the sector scan is at 123° and imaging is perpendicular to the coaptation line. In the bottom frame, the sector scan has been reduced to 94°. Imaging is now along the coaptation and results in marked broadening of the regurgitant jet. This finding suggests that the regurgitant orifice is elliptical in shape. Both frames were obtained a few seconds apart in the same patient. **(B)** In this case, reducing the sector scan from 134° (*top*) to 69° (*bottom*) results in the appearance of two regurgitant jets. The double jet is due to a single elliptical regurgitant orifice that is cut twice by the scan plane (see Figure 4C). Both frames were obtained a few seconds apart in the same patient.

Assessing Severity

Numerous quantitative and qualitative methods are used for assessing MR severity.[68] Discussion here is limited to three of the most important techniques that are applicable in the perioperative period: (1) vena contracta width (VCW), (2) estimation of effective regurgitant orifice area (EROA) by the flow convergence technique, and (3) vena contracta area (VCA). VCW and the flow convergence method are recommended in guidelines,[68-70] and VCA is an important emerging technique.

VCW. VCW is the most widely used method for assessing MR severity in the operating room. The technique can be performed rapidly, is relatively independent of machine settings, and provides a reproducible, semiquantitative assessment of severity in most patients.

The vena contracta is the narrowest part of the jet as it passes through the valve and should be measured perpendicular to the coaptation line, in the midesophageal long-axis view (Figure 14). The region of interest should be optimized using the depth or zoom function, and the Nyquist limit (NL) should be set to 40 to 70 cm/sec. The probe should be turned to the left (counterclockwise) and right (clockwise) to avoid missing jets in the A1/P1 and A3/P3 regions (Figure 4D). The narrowest part (the neck) of the widest jet should be used for analysis and the average of at least three measurements reported. In some patients, a vena contracta cannot be visualized, and even in the long-axis view, it can be difficult to be sure the image plane is perpendicular to the coaptation line. VCW can usually be estimated for eccentric jets, but the technique is not valid when there are multiple jets. VCW < 3 mm indicates mild MR and a value ≥ 7 mm defines severe MR; however, intermediate values (4–6 mm) are indeterminate for distinguishing mild from severe MR.[68-70]

Flow Convergence. Flow convergence is the primary quantitative echocardiographic technique for assessing MR severity and can be rapidly performed in the operating room in most patients.

Using color Doppler imaging of the flow convergence zone on the left ventricular side of the valve, the point at which the blood velocity exceeds the NL is identified by color aliasing. The region of color change is a hemisphere of constant known velocity (the NL), termed the proximal isovelocity surface area (PISA). Assuming that the base of the hemisphere (i.e., the undersurface of the closed mitral leaflets) is flat, the surface area of the PISA is given by $2\pi r^2$, where r is the PISA

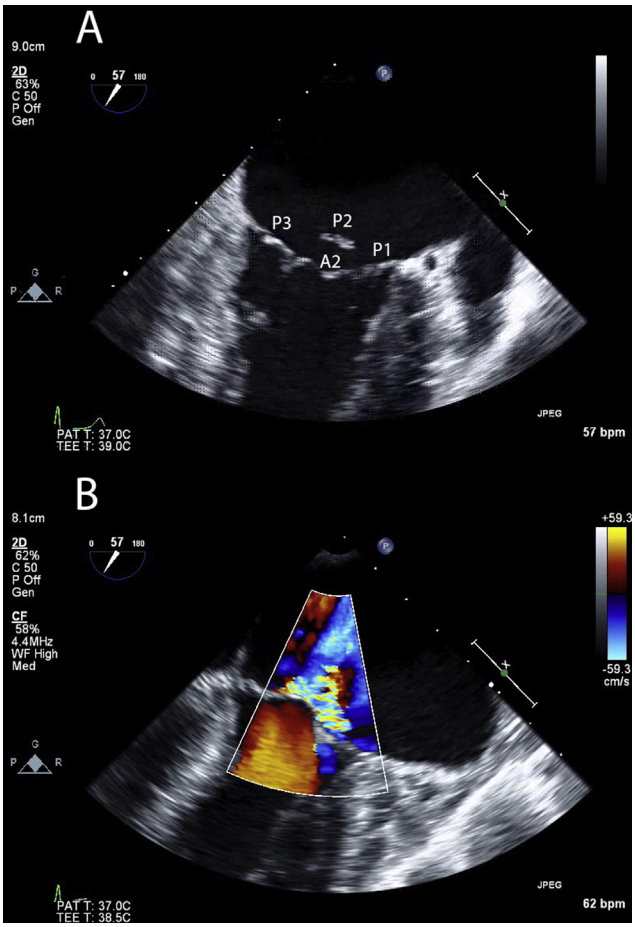

Figure 8 The cobra sign due to P2 flail. **(A)** With 2D imaging, the prolapsing P2 segment can be seen above the A2 segment (late systole, midesophageal commissural view). **(B)** With color flow Doppler, a broad jet of MR is seen above A2 (late systole, midesophageal commissural view).

radius. Flow at the PISA is equal to NL $\times$ $2\pi r^2$. Regurgitant flow through the orifice is the product of the peak mitral regurgitant jet velocity (V_{MR}) and EROA, the unknown quantity. Because flow at the PISA is the same as flow through the regurgitant orifice,

$$\text{EROA} = \frac{2\pi r^2 \times \text{NL}}{V_{MR}}$$

.

If the base of the mitral leaflets is not flat (i.e., $<180°$), the top line of the equation should be multiplied by $\alpha/180°$, where α is the angle subtended by the mitral leaflets.

Three parameters are required to calculate EROA (Figure 15): the PISA radius, the NL at which the PISA radius is measured, and V_{MR}, obtained with continuous-wave Doppler. When measuring V_{MR}, it is important to ensure that the Doppler signal is aligned with the regurgitant jet to avoid underestimating peak velocity (and therefore overestimating EROA). Accurate measurement of the PISA radius is essential, because this value is squared when calculating flow. A low NL (e.g., to 40 cm/sec) provides a large PISA radius and helps reduce measurement error. Underestimating PISA radius underestimates EROA. The technique assumes a symmetric PISA hemisphere, which implies a circular regurgitant orifice. The correction factor ($\alpha/180°$) is not usually necessary for degenerative MR but may be necessary with rheumatic heart disease or severe FMR, when systolic tethering imparts a conical shape to the regurgitant orifice. Failure to apply a correction factor when indicated overestimates severity. The PISA technique is more accurate for central jets than eccentric jets.

Organic MR is considered severe when the EROA is $\geq$40 mm^2 and mild when $<$20 mm^2.[68-70] Moderate MR can be subclassified as mild to moderate (EROA of 20–29 mm^2) or moderate to severe (EROA of 30–39 mm^2).

A simplified form of the flow convergence method may be used, in which the left ventricular–to–left atrial pressure difference is assumed to be 100 mm Hg (i.e., $V_{MR} \sim 5$ m/sec). Then, when the NL is set to 40 cm/sec, the formula for EROA simplifies to $r^2/2$. In this circumstance, a PISA radius of 10 mm indicates an EROA of 50 mm^2. This technique yields accurate measurements for EROA for a wide range of regurgitant severity[71] but is not applicable when left ventricular function is severely impaired, because V_{MR} is typically reduced.

VCA. VCA can be measured with quantitative analysis of 3D data sets (Figure 16) and provides a measure of the regurgitant orifice area. VCA has a particular advantage over VCW and the flow convergence method in that no assumptions are made regarding the shape of the regurgitant orifice.

To obtain 3D data sets suitable for measuring VCA, it is essential that the vena contracta be well visualized with standard color Doppler imaging before acquiring the data set. Poor temporal resolution (low frame rate) is a common problem with color 3D imaging. To maximize temporal resolution, the narrowest sector width that contains the vena contracta should be used, and the data set acquired over four to six beats. Cutoff values for regurgitant orifice area calculated by VCA have not been fully defined. However, using quantitative measurement of regurgitant volume as a reference, a VCA of 41 mm^2 differentiates moderate from severe MR with sensitivity of 97% and specificity of 82%.[72] Compared with the flow convergence method, VCA yields higher values for regurgitant orifice area, particularly for patients with FMR.[72]

Caveats and Considerations. Several factors must be considered when grading MR. First, severity is greatly influenced by the hemodynamic state, particularly for FMR. In general, MR severity is reduced by hypovolemia, hypotension, arteriolar vasodilation, and low cardiac output. Reduced preload and afterload associated with general anesthesia lead to a significant reduction in MR severity.[73,74] Before performing measurements, vasopressors and fluid should be administered to mimic the awake state. Systolic arterial blood pressure should increased to $>$140 mm Hg, unless this would be inappropriate (e.g., during surgical manipulations of the aorta). In patients in atrial fibrillation, in whom stroke volume varies from beat to beat, the average of at least five measurements should be reported.

Second, all three techniques rely on the analysis of a single frame, which may not be representative of the entire cardiac cycle. Indeed, for degenerative and FMR, regurgitant flow varies greatly throughout systole.[75,76] Regurgitant flow is primarily dependent on the transmitral pressure gradient (left ventricular–left atrial pressure difference) and EROA. With FMR, regurgitant flow and EROA are greatest in early systole. Flow typically reduces (and may cease) in midsystole and may be followed by a second, smaller, peak in late systole. With degenerative disease, regurgitant flow and EROA typically increase throughout systole, peaking in late systole

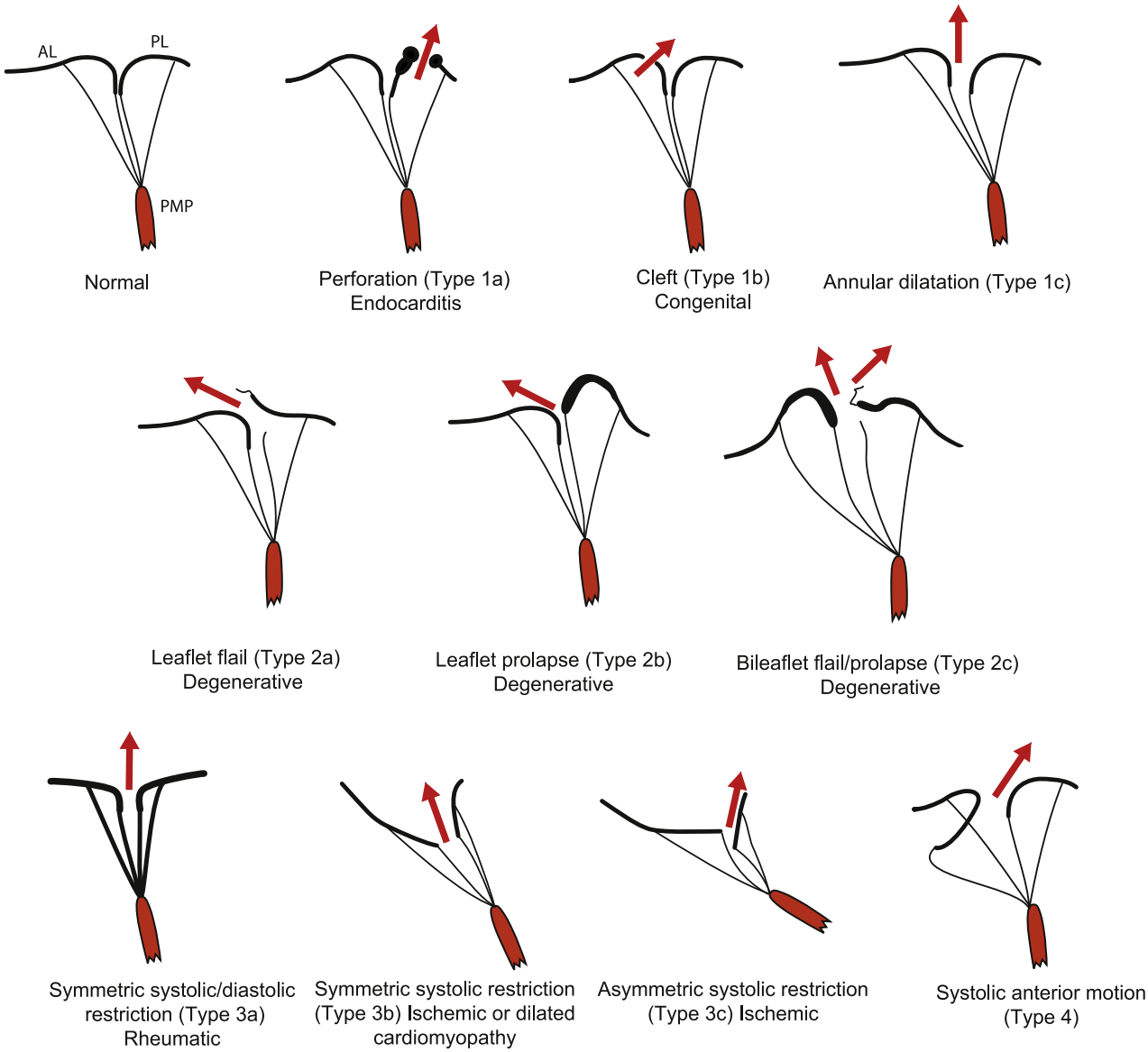

Figure 9 Echocardiographic classification of MV pathology on the basis of leaflet motion.[64] Arrows indicate the direction of the regurgitant jet. With type 1 pathology, there is normal leaflet motion, and regurgitation results from leaflet perforation (1a), cleft (1b), or a dilated annulus (1c). Type 2 refers to excessive leaflet motion and may be due to isolated flail (2a), isolated prolapse (2b), or bileaflet prolapse/flail (2c). Type 3 refers to restricted leaflet motion. Leaflet motion may be restricted in systole and diastole (3a), such as occurs with rheumatic disease, or limited to systole only, such as occurs with FMR. Systolic leaflet restriction may be further subclassified as symmetric (3b) or asymmetric (3c). Type 4 refers to SAM, which may be due to hypertrophic cardiomyopathy (4a), post-MV repair (4b), or be hemodynamic-induced (4c) (e.g., because of hypovolemia). Hybrid conditions (type 5) are also recognized; for instance, anterior leaflet prolapse in combination with posterior leaflet restriction. *AL*, Anterior mitral leaflet; *PL*, posterior mitral leaflet; *PMP*, posteromedial papillary muscle.

(Figure 17). There is no simple solution to the problem of when in the cardiac cycle to assess severity. When MR is highly dynamic, it is not possible to choose a representative frame. Thus, the frame demonstrating the most severe regurgitation is usually chosen. However, with dynamic MR, choosing the most severe frame overestimates severity compared with quantitative estimation of regurgitant volume.[77]

Third, both VCW and the flow convergence method assume a circular shape of the regurgitant orifice. Although this is generally the case for isolated leaflet prolapse or flail, it is not the case for FMR and for complex degenerative disease. In particular, with FMR, the jet is typically elliptical or slitlike, in which case VCW and the flow convergence method underestimate severity. By contrast, VCA does not underestimate severity for elliptical jets, and the technique is particularly useful for assessing FMR.[72,78,79] Because several individual VCAs can be summed, the technique is also valid when there are multiple jets.[60]

Considerations for FMR

On the basis of the foregoing discussion, it should be clear that FMR presents particular challenges to the perioperative echocardiographer.

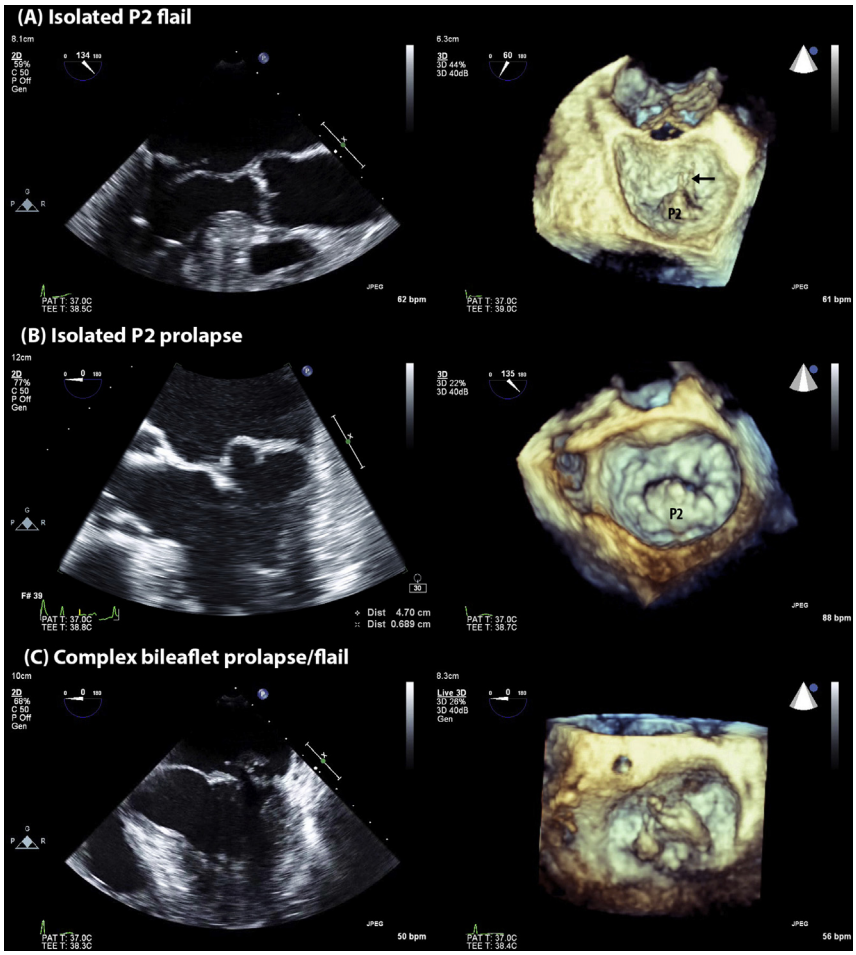

Figure 10 Spectrum of degenerative MV disease. **(A)** Isolated P2 flail. The flail segment is easily seen with 2D (midesophageal long-axis view) and 3D imaging. Additionally, in the 3D view, torn chordae (*arrow*) are identified. **(B)** Isolated P2 prolapse. With 2D imaging (midesophageal five-chamber view), the body of P2 domes above the annular plane at end-systole. (Normally, leaflets lie at or below the annular plane at end-systole). With 3D imaging, prolapse of the entire P2 segment is shown. **(C)** Complex prolapse/flail. Myxomatous change involving both leaflets is apparent with 2D imaging (midesophageal four-chamber view). With 3D imaging, predominant involvement of P2 is identified.

Quantification is difficult as severity is highly load dependent, regurgitant flow varies greatly throughout systole, and the regurgitant orifice is usually elliptical or slitlike. Additionally, for patients with FMR, an EROA > 20 mm^2 is an independent predictor of cardiac death,[80] and therefore EROA values > 20 mm^2 are used for defining severe FMR.[69,70] This finding may be partly technical, as a consequence of underestimating the severity of FMR using the flow convergence technique.[80]

Despite these problems, intraoperative quantification of FMR may be crucially important. In most circumstances, patients with FMR are scheduled for coronary artery bypass graft surgery, and MR may have been inadequately defined preoperatively or have changed since the preoperative assessment, particularly if postinfarction remodeling has occurred. Guidelines recommend that for patients undergoing coronary artery bypass graft surgery (with LVEF $> 30\%$), MV valve surgery be performed when MR is severe and be considered when MR is moderate.[70] Although guidelines recommend reducing the threshold for defining severe MR for the flow convergence method, no reduction is suggested for VCW,[69,70] despite the potential for underestimating severity with VCW also. VCA avoids the problem of underestimating regurgitant orifice area, but there are no FMR-specific thresholds recommended for this technique. Furthermore, for patients with severe leaflet tethering, MV repair has a high failure rate, and MV replacement may be a better technique. Thus, there is uncertainty both in quantifying moderate or severe FMR and then, once defined, deciding on the appropriate treatment.

When assessing FMR, careful assessment under "awake" loading conditions using more than one technique is appropriate. When possible, VCA should be measured. In general, FMR that is thought to be moderate or worse should be treated with an annuloplasty band. However, severe MR with marked leaflet tethering and annular dilatation may be better treated with MV replacement.

Left and Right Heart Function

MR imposes a volume load on the left ventricle, which leads to atrial and ventricular dilatation and elevated end-diastolic pressure. Initially, end-diastolic dimension increases but end-systolic dimension is maintained, resulting in increased LVEF and fractional area change. Increased end-systolic dimension (>35–40 mm) is indicative of impaired left ventricular systolic function and initially occurs despite "normal" values of LVEF and fractional area change.[13] End-systolic

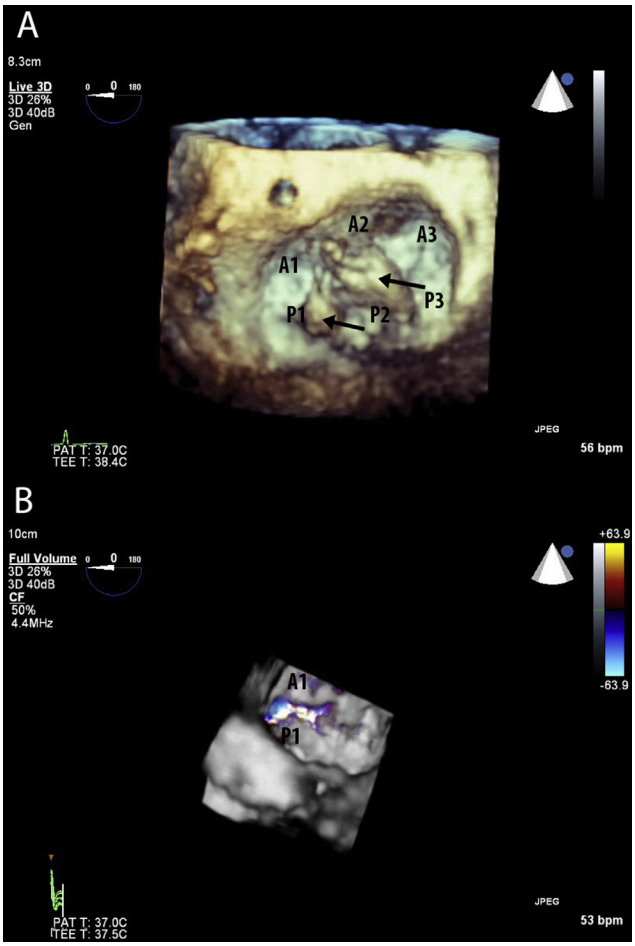

Figure 11 Three-dimensional imaging in a patient with complex degenerative MV disease. **(A)** On standard 3D imaging, two regions of prolapse/flail (*arrows*) can be seen involving the posterior leaflet. **(B)** With color 3D imaging, the site of regurgitation is identified as involving only A1/P1 segments.

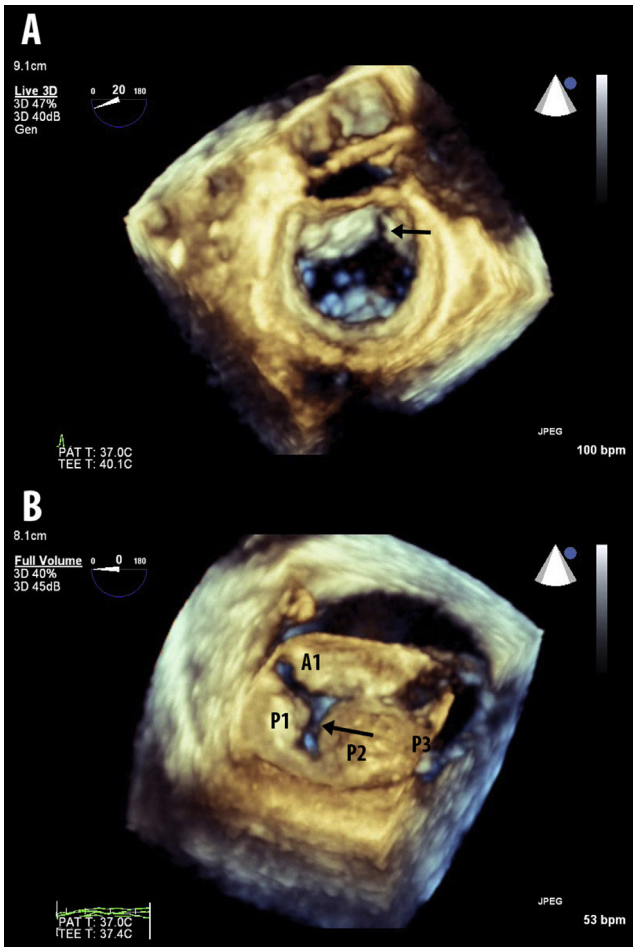

Figure 12 Mitral clefts. **(A)** Anterior leaflet cleft (*arrow*) involving A2/A3. **(B)** Posterior leaflet cleft involving P1/P2. The cleft is in the region of the scallop that normally separates P1 and P2 and therefore may be considered a "deep scallop."

and end-diastolic areas and fractional area change are conveniently measured in the transgastric mid-short-axis view.

Increased left atrial pressure leads to pulmonary hypertension. Initially, pulmonary hypertension is due to passive back pressure from the left atrium and is therefore mild. However, overtime, pulmonary hypertension may become severe because of microvascular changes in the pulmonary circulation leading to increased pulmonary vascular resistance (PVR). Elevated PVR causes right ventricular pressure overload, which can lead to right ventricular failure and functional TR. The right ventricle is best assessed in a modified midesophageal four-chamber view, with the image centered on the right heart. Signs of right ventricular pressure overload include ventricular hypertrophy and dilatation, increased muscular trabeculations, impaired systolic function, and an elevated maximal TR jet velocity (>3 m/sec). The absence of elevated maximal TR jet velocity in the presence of severe TR suggests intrinsic tricuspid valve disease (e.g., endocarditis or rheumatic heart disease). However, the absence of high TR velocity can also occur when TR is torrential, because of the nonrestrictive regurgitant orifice being too large to create a right atrial–to–right ventricular gradient (the "single-chamber" effect).

A standard approach to measuring the tricuspid annular dimension with TEE has not been established. Using transthoracic echocardiographic criteria, the upper limit of normal for the tricuspid annulus is 33 mm measured in an apical four-chamber view in late diastole, with values > 40 mm indicative of significant dilatation.[69,70] With TEE, similar cutoff values may be used from the midesophageal four-chamber view with the image centered on the right heart and calipers placed on the hinge points of the leaflets. (In contrast to the mitral annulus, which is measured at end-systole,[63] the tricuspid annulus is typically measured in late diastole.)

TR should be assessed in multiple views, as it may not be apparent in one view but obvious in another. VCW > 7 mm (four-chamber view) and PISA radius > 9 mm at an NL of 28 cm/sec are indicative of severe TR.[68,70]

There is debate as to the appropriate intervention for functional TR, but in general, a tricuspid annuloplasty should be placed at the time of MV surgery in patients with severe TR or moderate TR with a dilated annulus (>40 mm).[69,70]

EXAMINATION AFTER CARDIOPULMONARY BYPASS

After separation from CPB, the focus of the transesophageal echocardiographic examination is to determine the mechanism and severity

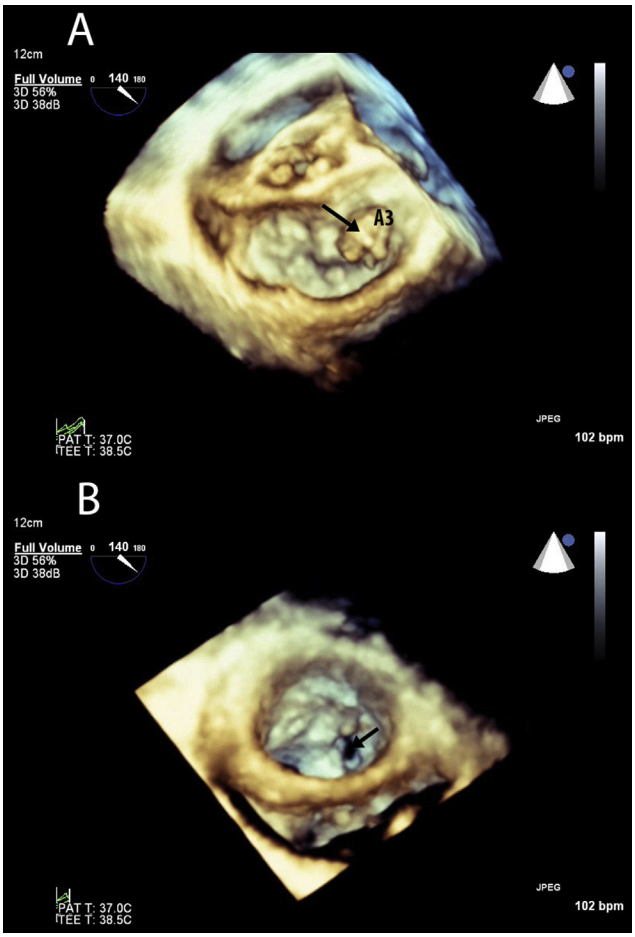

Figure 13 Mitral endocarditis. **(A)** A large vegetation (*arrow*) can be seen in the region of A3. The MV is shown in the surgical orientation. **(B)** The 3D data set has been flipped over to display the MV from the left ventricular aspect. A perforation (*arrow*) can be seen in the A3 segment, which was hidden by the vegetation in the top image.

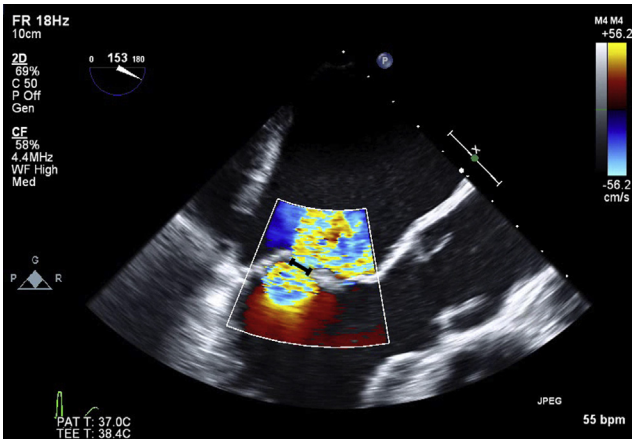

Figure 14 Measurement of VCW. The vena contracta is identified at the level of the mitral orifice in late systole in the midesophageal long-axis view. A large proximal flow convergence zone is seen on the left ventricular side of the valve, and a broad regurgitant jet is present in the left atrium.

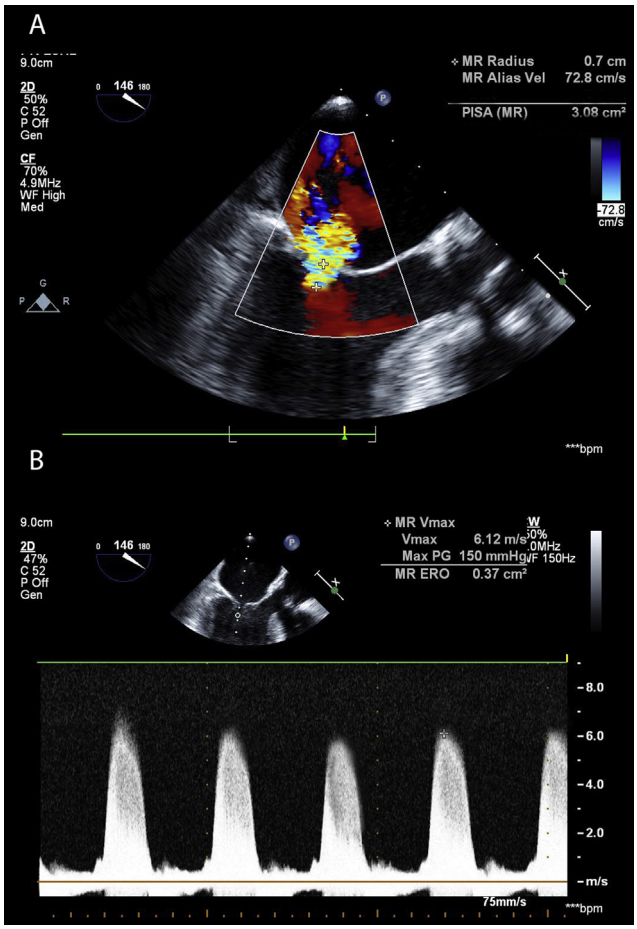

Figure 15 Measurement of the EROA by the flow convergence method. **(A)** Color Doppler imaging demonstrating a flow convergence zone on the left ventricular side of the valve in late systole (midesophageal long-axis view). The PISA radius is measured from the tip of the mitral leaflets in late systole to the point of first aliasing. **(B)** Continuous-wave Doppler imaging through the mitral leaflets demonstrating the peak regurgitant velocity of the regurgitant jet (midesophageal long-axis view). In this example, the PISA radius is 7 mm, the NL is 72.8 cm/sec, and V_{MR} is 6.12 m/sec, yielding an EROA of 37 mm^2 (i.e., moderate to severe MR).

of any residual MR, to exclude clinically significant mitral stenosis or SAM, and to assess ventricular function.

The primary goal of any repair technique is to restore an adequate coaptation surface. A durable repair is associated with a coaptation height $>$ 8 mm.[81] An annuloplasty band should be placed in all patients to increase coaptation height, correct annular dilatation, and prevent further dilatation.[81,82] Leaflet motion, coaptation height, and correct seating of the annuloplasty band should be assessed in the midesophageal long-axis view, with measurements made at end-systole. Even in the absence of any residual MR, reduced coaptation height and residual prolapse or tethering should be discussed with the surgeon.

Repair-Specific Echocardiographic Appearances

Annuloplasty rings may be complete or partial, the latter being deficient anteriorly in the region of the intervalvular fibrosa. The annuloplasty band is usually easily visualized with echocardiography.

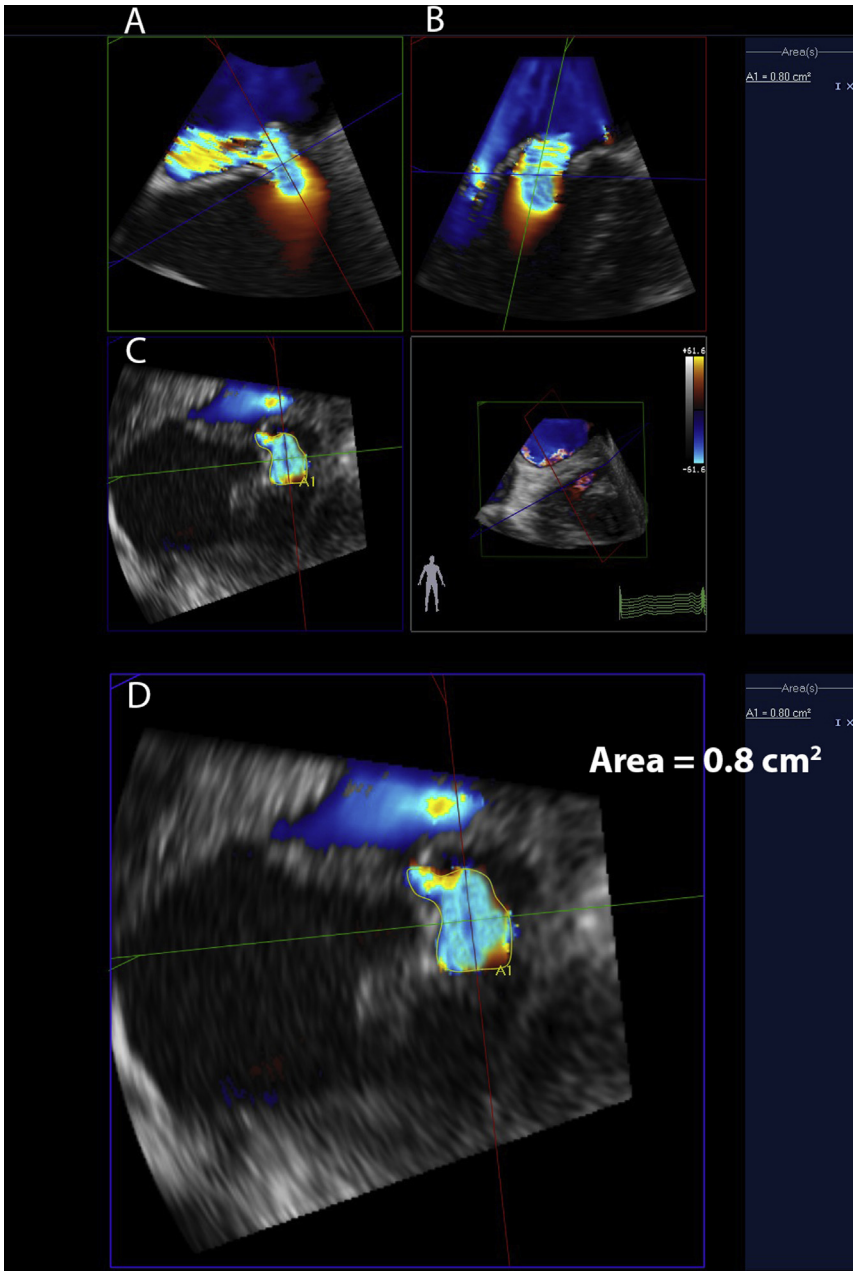

Figure 16 Measurement of VCA with quantitative 3D imaging. The 3D data set is displayed in three simultaneous, adjustable, orthogonal 2D planes (coronal, sagittal, and transverse, or x, y, and z). The x and y planes (**A** and **B**, respectively) are aligned to the long axis of the regurgitant jet. The z plane **(C,D)** is adjusted to ensure that it is perpendicular to the jet and then moved along the jet direction until it passes through the smallest jet area, which is the vena contracta. VCA is then measured by planimetry (labeled A1 in **C** and **D**), which in this example is 80 mm^2, indicating severe regurgitation.

The classic repair technique for degenerative disease of the posterior leaflet is to resect prolapsing or flail segments and their associated chordae (Figure 18A). For limited prolapse or flail, a simple triangular resection is performed. For more extensive leaflet prolapse or flail, a quadrangular resection and annular plication are required. With posterior leaflet resection, echo dropout from the annuloplasty ring makes visualizing the residual posterior leaflet difficult, creating the appearance of a unicuspid valve.

An alternative approach to leaflet resection, which may be used for both anterior and posterior leaflet repairs, is to replace ruptured or elongated chordae with polytetrafluoroethylene neochordae (Figure 18B).[81,83] Typically, the goal is to return the plane of coaptation to the level of the mitral annulus. However, when there is bulky or excess tissue, shortened neochordae may be used to displace the prolapsing or flail segment(s) into the left ventricle. With this approach, the plane of coaptation may lie below the annular plane. Neochordae are more echogenic than native chordae.

Residual Regurgitation

Assessment of residual MR (Figure 19) should be performed once the left ventricle has recovered from the effects of CPB and once

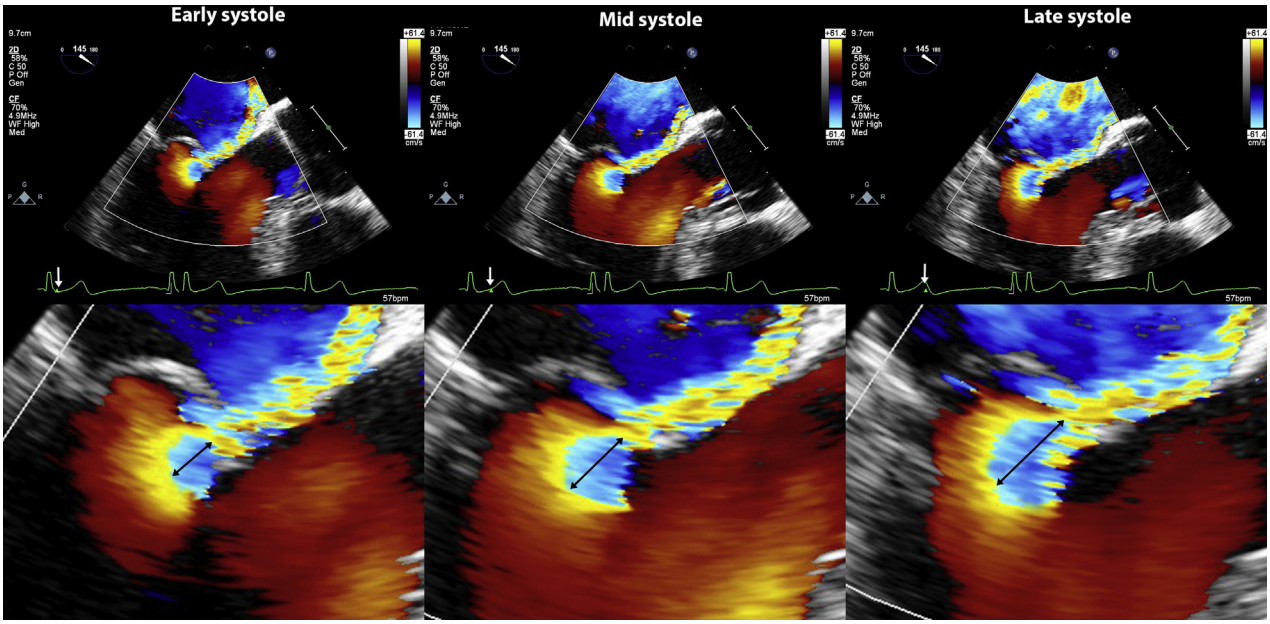

Figure 17 Increase in the radius of the PISA with color flow Doppler imaging from early to late systole in a patient with severe MR due to leaflet prolapse/flail. The increase in PISA radius (*arrow*) is reflective of increasing regurgitant orifice area. See text for details.

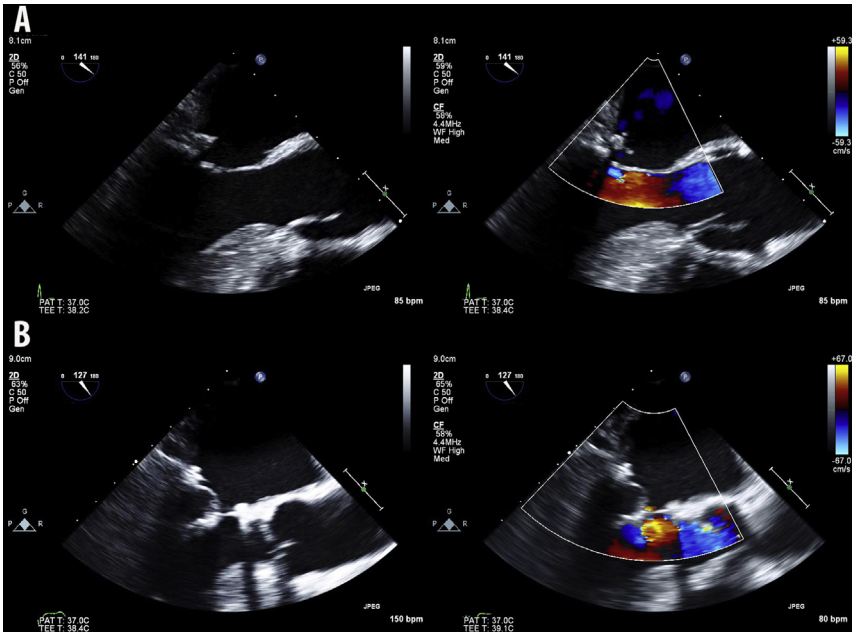

Figure 18 Typical echocardiographic appearances after MV repair. **(A)** Appearances after quadrangular resection for P2 prolapse (late systole, midesophageal long axis view). With 2D imaging (*left frame*), a short bulky posterior leaflet is seen, and there is an apparent systolic coaptation defect. The bulky appearance is due to the annuloplasty band, and the apparent coaptation defect is due to echocardiographic dropout from the annuloplasty band, obscuring the coaptation point. Thus, coaptation height cannot be assessed. In this case, a partial annuloplasty band has been used. No MR is evident with color Doppler imaging (*right*), despite the apparent coaptation defect (due to echocardiographic dropout). **(B)** Appearances after placement of neochordae for P2 flail (late systole, midesophageal long-axis view). With 2D imaging (*left*), the posterior leaflet is well seen, and the coaptation height is obviously satisfactory. The annuloplasty ring is well seen posteriorly and anteriorly. With color Doppler imaging (*right*), a trivial amount of MR is seen.

appropriate inotropic, vasopressor, and fluid therapy has been administered. VCW is the most useful technique for rapidly quantifying the severity of residual regurgitation, and 3D (with and without color Doppler) imaging is useful for identifying the anatomic location. Flow convergence is often less useful for defining residual MR, as the PISA is not well formed or is too small to measure when MR is mild.

Residual regurgitation that is more than mild is an indication to revise the repair or replace the valve because of an increased need

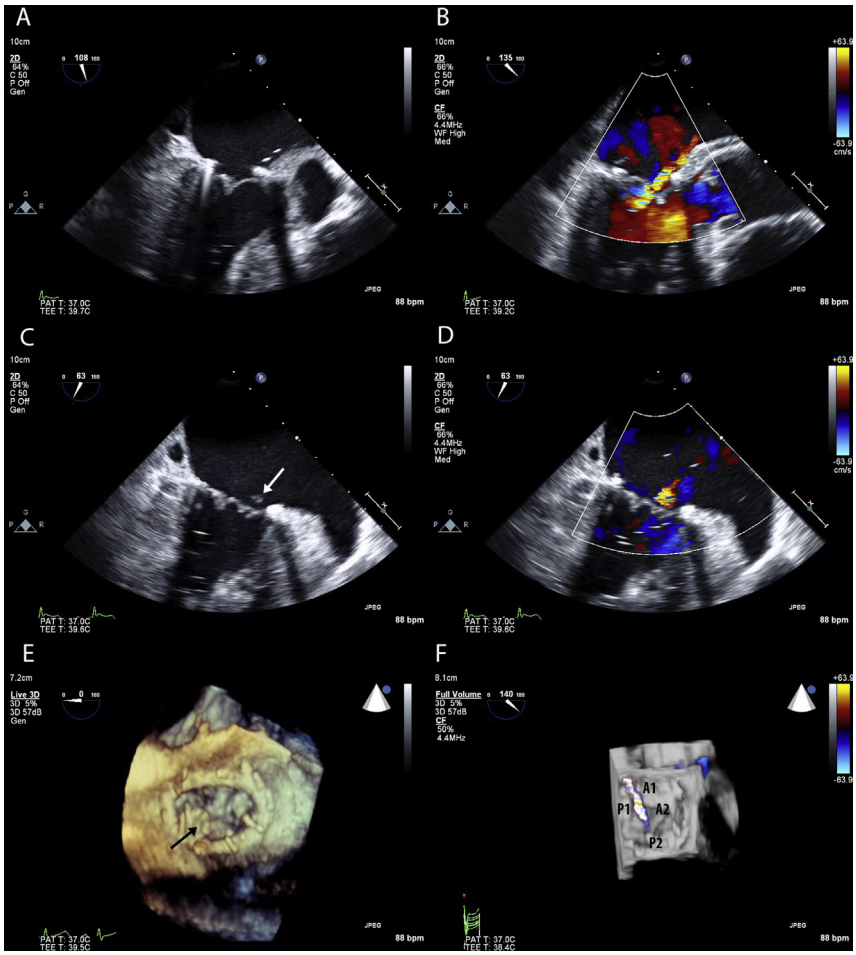

Figure 19 Residual MR due to uncorrected leaflet prolapse. The operative procedure consisted of a triangular resection of P2 and placement of an annuloplasty ring. **(A,B)** There is minimal leaflet coaptation, and a jet of MR can be seen (late systole, midesophageal long-axis view). **(C,D)** There is residual leaflet prolapse (*arrow*), associated with a small regurgitant jet, which can be localized to P1/A1 (late systole, midesophageal commissural view). **(E,F)** On 3D imaging, residual prolapse (*arrow*) can be seen in the P1 region. On color 3D imaging, the residual regurgitation is clearly localized to the P1/A1 region (late systole, 3D en face view, surgical orientation).

for reoperation.[22,84,85] However, few studies have examined the consequences of untreated mild residual MR. Meyer *et al.*[84] found that more than trivial MR was an independent risk factor for reoperation but did not distinguish mild from moderate regurgitation. Despite limited data, the goal at most experienced centers is to achieve nil or trivial residual regurgitation. The decision to revise a repair for mild MR must be individualized taking into consideration the likelihood of improving the repair, the risks of a second CPB run, and the potential risk for subsequent reoperation.

Although the distinction between trivial and mild MR is usually straightforward, differentiating mild from moderate MR can be difficult. VCW may vary depending on the image plane and the point in the cardiac cycle, straddling the cutoff (3 mm) between mild and moderate regurgitation. Carefully turning the probe left and right in the midesophageal long-axis view ensures that the entire coaptation line is imaged. It is not uncommon to see a brief jet of regurgitation that is present only in early systole and does not extend far into the left atrium. Such jets frequently disappear after a few minutes. In difficult cases, it is appropriate to wait for up to 30 min after separation from CPB before making a final decision on revision, as we have observed significant and sustained reductions in residual MR during this period, presumably related to recovery of left ventricular function.

Common causes for residual MR are uncorrected prolapse (Figure 19), excessive leaflet tension causing separation of the posterior scallops,[86] inadequate coaptation height, persistent leaflet tethering, uncorrected clefts or perforations, leaflet perforation from the annuloplasty band, and SAM. Turbulent jets occurring outside the annuloplasty band indicate leaflet perforation; such jets, even if trivial, should be corrected as they may progress or cause hemolysis.

Mitral Stenosis

Clinically significant stenosis is rare but is occasionally seen when a small annuloplasty ring has been placed and extensive commissural plication has been performed. The MV should be assessed with 2D and color Doppler imaging, looking for restricted diastolic leaflet excursion and a flow convergence zone on the left atrial side of the valve during diastole. Transvalvular pressure gradients should be measured with continuous-wave Doppler. However, assessment of postrepair mitral stenosis is complicated by the fact that diastolic pressure gradients are typically higher in the early postoperative period than at subsequent

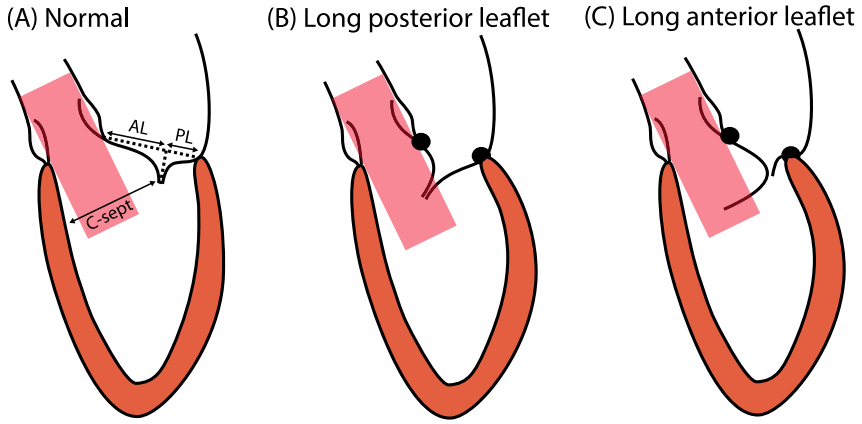

Figure 20 Schematic demonstrating the mechanisms of SAM. **(A)** Prerepair echocardiographic measurements that are predictive of SAM are indicated. When measuring the ratio of anterior leaflet (AL) to posterior leaflet (PL) length, the leaflets should be measured along the annular plane at end-systole. See text for details. **(B)** Effect of a long PL. A long PL, in combination with an undersized annuloplasty ring, displaces the coaptation line anteriorly and pushes the anterior mitral leaflet into the LVOT. This is the classical mechanism for postrepair SAM. The *shaded pink* area represents systolic blood flow into the LVOT. **(C)** Effect of a long AL. A long AL, in combination with an undersized annuloplasty ring, can also result in the AL's being exposed to the LVOT, with resultant SAM. Image modified from Kahn RA, Mittnacht AJ, Anyanwu AC. Systolic anterior motion as a result of relative "undersizing" of the mitral valve annulus in a patient with Barlow's disease. Anesth Analg 2009:108:1102-1104. *C-sept*, Shortest distance from the coaptation point to the anterior ventricular septum at end-systole.

follow-up because of the hyperdynamic circulation after CPB. The transvalvular pressure gradient is also exacerbated by tachycardia. Mean diastolic gradients of 3 to 5 mm Hg are not uncommon in the early postrepair period. There are few data to guide decision making; however, in one study of 552 patients undergoing MV repair, a mean diastolic pressure gradient of 7 mm Hg and a peak gradient $\geq$ 17 mm Hg reliably identified the need for reoperation.[87]

SAM

SAM is the movement of the anterior mitral leaflet into the LVOT during systole, resulting in LVOT obstruction and MR. The clinical manifestation of SAM is highly variable, ranging from entrainment of only the tip of the anterior mitral leaflet in late systole with no MR to intractable LVOT obstruction and severe MR. This clinical variability may partly explain the wide range in reported incidence of between 1% and 16%.[88]

The mechanism of postrepair SAM is complex and involves anatomic and hemodynamic factors. However, fundamentally, SAM is explained by the presence of excess leaflet tissue relative to annular size. Blood flowing through the LVOT in systole creates drag forces on the mitral leaflets. Excessive leaflet tissue predisposes to SAM by creating a larger surface area on which drag forces act.[88] Both excessive anterior[89,90] and posterior[91] leaflet tissue predispose to SAM (Figure 20); however, a long posterior relative to anterior leaflet length, in which the coaptation line is displaced anteriorly into the LVOT, is a particular risk factor. On the prerepair transesophageal echocardiographic examination, the risk for SAM is increased with an anterior-to-posterior leaflet length ratio $<$ 1.3 and a distance from the coaptation point to the septum $<$ 25 mm (Figure 20).[92] Other anatomic risk factors are a nonenlarged annulus, hypertrophy of the basal anterior ventricular septum, and a small left ventricle.[88] Hypovolemia, increased left ventricular contractility, and low left ventricular afterload also predispose to SAM by increasing the blood velocity within and reducing the diameter of the LVOT.

For patients at increased risk for SAM, several surgical strategies may be used. Avoiding undersizing of the annuloplasty ring is very important in patients with excess leaflet tissue. If the anterior leaflet is very bulky, an elliptical excision of the body of the anterior leaflet may be performed[93,94] and the annuloplasty sized according to the new anterior leaflet length. For excess posterior leaflet tissue, a sliding valvuloplasty may be performed, in which, in addition to a triangular resection, a strip of tissue along the posterior mitral annulus is resected to reduce the length of the posterior leaflet.[95] Displacing bulky posterior leaflet tissue into the left ventricle with shortened neochordae helps minimize SAM by moving the coaptation point posteriorly, away from the LVOT.

SAM is best seen in the midesophageal long-axis view and has a characteristic appearance on 2D, color Doppler, and continuous-wave Doppler imaging (Figure 21). The appropriate intervention for SAM depends on its severity and response to medical therapy. SAM that is associated with a normal LVOT velocity ($<$2 m/sec) and minimal MR can be ignored. In the first instance, more severe forms of SAM should be treated with volume loading, vasoconstrictors, and cessation of inotropes. If, despite these measures, the LVOT velocity remains $>$3.5 m/sec and MR remains mild or greater, the repair should be revised.[96] However, surgical revision is only rarely required. In one series of 608 patients undergoing mitral repair, of the 60 patients who developed SAM, only four required reoperation.[97]

Left and Right Heart Function

Correction of severe MR increases left ventricular afterload and may unmask or exacerbate left ventricular systolic dysfunction. Thus, left ventricular dysfunction is common during the early postoperative period. Injury to the circumflex coronary artery, which lies adjacent to the anterolateral annulus (Figure 2), is a rare but important complication.[98] Circumflex artery injury can arise from a misplaced annuloplasty suture or distortion from the ring itself. Segmental wall motion abnormalities involving the basal and mid inferolateral walls of the left ventricle are likely to be present.

Right ventricular impairment may arise from several mechanisms, including gas embolus to the right coronary artery, poor myocardial

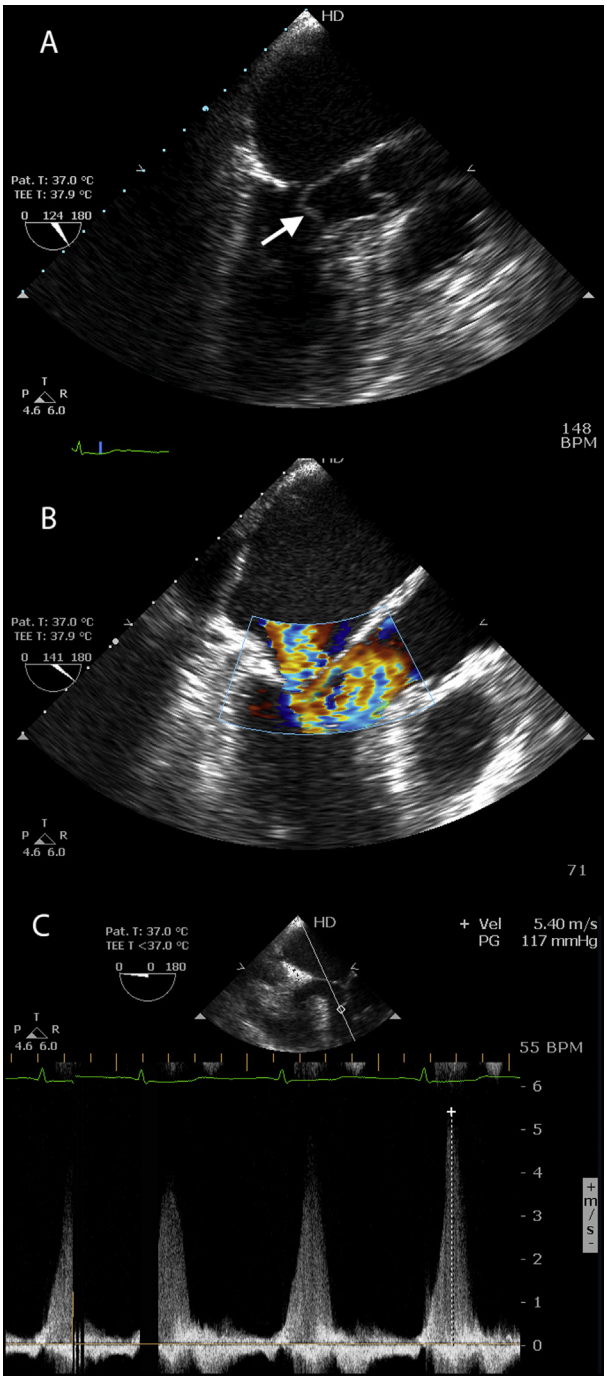

Figure 21 Characteristic appearances of SAM after MV repair. **(A)** With 2D imaging, there is characteristic bending of the anterior mitral leaflet (*arrow*) into the LVOT (late systole, midesophageal long-axis view). **(B)** With color flow Doppler imaging, there is marked turbulence in the LVOT, and a broad jet of MR is seen (late systole, midesophageal long-axis view). Although not obvious in this view, the regurgitant jet is usually posteriorly directed. **(C)** On continuous-wave (CW) Doppler imaging, a narrow, high-velocity (5.4 m/sec) regurgitant jet is seen, characteristic of SAM (late systole, midesophageal five-chamber view). Although not apparent in this view, the regurgitant jet is typically late peaking (i.e., maximal in late systole). Note that because the regurgitant jet is shown in the midesophageal five-chamber view, the CW signal is shown above the baseline (i.e., toward the transducer).

protection, and acute or chronic elevations in PVR. Gas embolus is a particular concern during minimally invasive MV repair when de-airing of the heart is more difficult than with open procedures. Functional TR may develop or worsen because of impaired right ventricular systolic function, elevated PVR, and failed tricuspid valve repair.

CONCLUSIONS

Surgical repair of MR, particularly for degenerative disease, is both effective and durable. Recent developments in surgical technique, notably the increased use of complex bileaflet repairs and the growth of minimally invasive approaches, have increased surgical reliance on TEE and placed additional demands on perioperative echocardiographers. A thorough understanding of the function of normal and abnormal MVs, along with an appreciation of the benefits and limitations of different echocardiographic views and imaging techniques, is essential for good patient care. Despite the challenges, expert transesophageal echocardiographic imaging during MV repair facilitates good surgery, improves patient outcomes, and is highly rewarding.

REFERENCES

1. Gammie JS, Sheng S, Griffith BP, Peterson ED, Rankin JS, O'Brien SM, et al. Trends in mitral valve surgery in the United States: results from the Society of Thoracic Surgeons Adult Cardiac Surgery Database. Ann Thorac Surg 2009;87:1431-7.
2. Badhwar V, Peterson ED, Jacobs JP, He X, Brennan JM, O'Brien SM, et al. Longitudinal outcome of isolated mitral repair in older patients: results from 14,604 procedures performed from 1991 to 2007. Ann Thorac Surg 2012;94:1870-9.
3. Shuhaiber J, Anderson RJ. Meta-analysis of clinical outcomes following surgical mitral valve repair or replacement. Eur J Cardiothorac Surg 2007;31:267-75.
4. Practice guidelines for perioperative transesophageal echocardiography. A report by the American Society of Anesthesiologists and the Society of Cardiovascular Anesthesiologists Task Force on Transesophageal Echocardiography. Anesthesiology 1996;84:986-1006.
5. Practice guidelines for perioperative transesophageal echocardiography. An updated report by the American Society of Anesthesiologists and the Society of Cardiovascular Anesthesiologists Task Force on Transesophageal Echocardiography. Anesthesiology 2010;112:1084-96.
6. Silbiger JJ, Bazaz R. Contemporary insights into the functional anatomy of the mitral valve. Am Heart J 2009;158:887-95.
7. Padala M, Hutchison RA, Croft LR, Jimenez JH, Gorman RC, Gorman JH III, et al. Saddle shape of the mitral annulus reduces systolic strains on the P2 segment of the posterior mitral leaflet. Ann Thorac Surg 2009;88:1499-504.
8. Salgo IS, Gorman JH III, Gorman RC, Jackson BM, Bowen FW, Plappert T, et al. Effect of annular shape on leaflet curvature in reducing mitral leaflet stress. Circulation 2002;106:711-7.
9. Silbiger JJ. Anatomy, mechanics, and pathophysiology of the mitral annulus. Am Heart J 2012;164:163-76.
10. Grewal J, Suri R, Mankad S, Tanaka A, Mahoney DW, Schaff HV, et al. Mitral annular dynamics in myxomatous valve disease: new insights with real-time 3-dimensional echocardiography. Circulation 2010;121:1423-31.
11. Shanks M, Delgado V, Ng AC, van der Kley F, Schuijf JD, Boersma E, et al. Mitral valve morphology assessment: three-dimensional transesophageal echocardiography versus computed tomography. Ann Thorac Surg 2010;90:1922-9.

12. Carpentier AF, Lessana A, Relland JY, Belli E, Mihaileanu S, Berrebi AJ, et al. The "physio-ring": an advanced concept in mitral valve annuloplasty. Ann Thorac Surg 1995;60:1177-85.
13. Enriquez-Sarano M, Akins CW, Vahanian A. Mitral regurgitation. Lancet 2009;373:1382-94.
14. Gupta V, Barzilla JE, Mendez JS, Stephens EH, Lee EL, Collard CD, et al. Abundance and location of proteoglycans and hyaluronan within normal and myxomatous mitral valves. Cardiovasc Pathol 2009;18:191-7.
15. Han RI, Black A, Culshaw G, French AT, Corcoran BM. Structural and cellular changes in canine myxomatous mitral valve disease: an image analysis study. J Heart Valve Dis 2010;19:60-70.
16. Anyanwu AC, Adams DH. Etiologic classification of degenerative mitral valve disease: Barlow's disease and fibroelastic deficiency. Semin Thorac Cardiovasc Surg 2007;19:90-6.
17. Adams DH, Anyanwu AC. Seeking a higher standard for degenerative mitral valve repair: begin with etiology. J Thorac Cardiovasc Surg 2008; 136:551-6.
18. Eriksson MJ, Bitkover CY, Omran AS, David TE, Ivanov J, Ali MJ, et al. Mitral annular disjunction in advanced myxomatous mitral valve disease: echocardiographic detection and surgical correction. J Am Soc Echocardiogr 2005;18:1014-22.
19. Chandra S, Salgo IS, Sugeng L, Weinert L, Tsang W, Takeuchi M, et al. Characterization of degenerative mitral valve disease using morphologic analysis of real-time three-dimensional echocardiographic images: objective insight into complexity and planning of mitral valve repair. Circ Cardiovasc Imaging 2011;4:24-32.
20. Levack MM, Jassar AS, Shang EK, Vergnat M, Woo YJ, Acker MA, et al. Three-dimensional echocardiographic analysis of mitral annular dynamics: implication for annuloplasty selection. Circulation 2012;126: S183-8.
21. David TE, Ivanov J, Armstrong S, Christie D, Rakowski H. A comparison of outcomes of mitral valve repair for degenerative disease with posterior, anterior, and bileaflet prolapse. J Thorac Cardiovasc Surg 2005;130: 1242-9.
22. Mohty D, Orszulak TA, Schaff HV, Avierinos JF, Tajik JA, Enriquez-Sarano M. Very long-term survival and durability of mitral valve repair for mitral valve prolapse. Circulation 2001;104:I1-7.
23. Johnston DR, Gillinov AM, Blackstone EH, Griffin B, Stewart W, Sabik JF III, et al. Surgical repair of posterior mitral valve prolapse: implications for guidelines and percutaneous repair. Ann Thorac Surg 2010; 89:1385-94.
24. Mihaljevic T, Jarrett CM, Gillinov AM, Williams SJ, DeVilliers PA, Stewart WJ, et al. Robotic repair of posterior mitral valve prolapse versus conventional approaches: potential realized. J Thorac Cardiovasc Surg 2011;141:72-80.
25. Seeburger J, Borger MA, Doll N, Walther T, Passage J, Falk V, et al. Comparison of outcomes of minimally invasive mitral valve surgery for posterior, anterior and bileaflet prolapse. Eur J Cardiothorac Surg 2009;36: 532-8.
26. Castillo JG, Anyanwu AC, Fuster V, Adams DH. A near 100% repair rate for mitral valve prolapse is achievable in a reference center: implications for future guidelines. J Thorac Cardiovasc Surg 2012;144:308-12.
27. Otsuji Y, Levine RA, Takeuchi M, Sakata R, Tei C. Mechanism of ischemic mitral regurgitation. J Cardiol 2008;51:145-56.
28. He S, Fontaine AA, Schwammenthal E, Yoganathan AP, Levine RA. Integrated mechanism for functional mitral regurgitation: leaflet restriction versus coapting force: in vitro studies. Circulation 1997;96:1826-34.
29. Kumanohoso T, Otsuji Y, Yoshifuku S, Matsukida K, Koriyama C, Kisanuki A, et al. Mechanism of higher incidence of ischemic mitral regurgitation in patients with inferior myocardial infarction: quantitative analysis of left ventricular and mitral valve geometry in 103 patients with prior myocardial infarction. J Thorac Cardiovasc Surg 2003;125: 135-43.
30. Gorman JH III, Jackson BM, Gorman RC, Kelley ST, Gikakis N, Edmunds LH Jr. Papillary muscle discoordination rather than increased annular area facilitates mitral regurgitation after acute posterior myocardial infarction. Circulation 1997;96:II-124-7.
31. Gorman JH III, Gorman RC, Plappert T, Jackson BM, Hiramatsu Y, St John-Sutton MG, et al. Infarct size and location determine development of mitral regurgitation in the sheep model. J Thorac Cardiovasc Surg 1998; 115:615-22.
32. Nass O, Rosman H, al-Khaled N, Shimoyama H, Alam M, Sabbah HN, et al. Relation of left ventricular chamber shape in patients with low (< or = 40%) ejection fraction to severity of functional mitral regurgitation. Am J Cardiol 1995;76:402-4.
33. Yiu SF, Enriquez-Sarano M, Tribouilloy C, Seward JB, Tajik AJ. Determinants of the degree of functional mitral regurgitation in patients with systolic left ventricular dysfunction: a quantitative clinical study. Circulation 2000;102:1400-6.
34. Vergnat M, Jassar AS, Jackson BM, Ryan LP, Eperjesi TJ, Pouch AM, et al. Ischemic mitral regurgitation: a quantitative three-dimensional echocardiographic analysis. Ann Thorac Surg 2011;91:157-64.
35. Vohra HA, Whistance RN, Magan A, Sadeque SA, Livesey SA. Mitral valve repair for severe mitral regurgitation secondary to lone atrial fibrillation. Eur J Cardiothorac Surg 2012;42:634-7.
36. Kongsaerepong V, Shiota M, Gillinov AM, Song JM, Fukuda S, McCarthy PM, et al. Echocardiographic predictors of successful versus unsuccessful mitral valve repair in ischemic mitral regurgitation. Am J Cardiol 2006;98:504-8.
37. Lee LS, Kwon MH, Cevasco M, Schmitto JD, Mokashi SA, McGurk S, et al. Postoperative recurrence of mitral regurgitation after annuloplasty for functional mitral regurgitation. Ann Thorac Surg 2012;94:1211-6.
38. Acker MA, Parides MK, Perrault LP, Moskowitz AJ, Gelijns AC, Voisine P, et al. Mitral-valve repair versus replacement for severe ischemic mitral regurgitation. N Engl J Med 2014;370:23-32.
39. Ciarka A, Braun J, Delgado V, Versteegh M, Boersma E, Klautz R, et al. Predictors of mitral regurgitation recurrence in patients with heart failure undergoing mitral valve annuloplasty. Am J Cardiol 2010;106:395-401.
40. Choudhary SK, Talwar S, Dubey B, Chopra A, Saxena A, Kumar AS. Mitral valve repair in a predominantly rheumatic population. Long-term results. Tex Heart Inst J 2001;28:8-15.
41. Chauvaud S, Fuzellier JF, Berrebi A, Deloche A, Fabiani JN, Carpentier A. Long-term (29 years) results of reconstructive surgery in rheumatic mitral valve insufficiency. Circulation 2001;104:I12-5.
42. Gao C, Xiao C, Li B. Mitral valve aneurysm with infective endocarditis. Ann Thorac Surg 2004;78:2171-3.
43. Tewari S, Moorthy N, Sinha N. Ruptured mitral valve aneurysm: an uncommon cause of acute dyspnoea. Echocardiography 2010;27:E119-21.
44. Wong PS, Yang H, Ling LH. Severe mitral regurgitation caused by annular abscess fistulating into the left atrium. Heart 2005;91:790.
45. Iung B, Rousseau-Paziaud J, Cormier B, Garbarz E, Fondard O, Brochet E, et al. Contemporary results of mitral valve repair for infective endocarditis. J Am Coll Cardiol 2004;43:386-92.
46. Zhu D, Bryant R, Heinle J, Nihill MR. Isolated cleft of the mitral valve: clinical spectrum and course. Tex Heart Inst J 2009;36:553-6.
47. Wyss CA, Enseleit F, van der Loo B, Grunenfelder J, Oechslin EN, Jenni R. Isolated cleft in the posterior mitral valve leaflet: a congenital form of mitral regurgitation. Clin Cardiol 2009;32:553-60.
48. McCarthy KP, Ring L, Rana BS. Anatomy of the mitral valve: understanding the mitral valve complex in mitral regurgitation. Eur J Echocardiogr 2010;11:i3-9.
49. Chen Q, Darlymple-Hay MJ, Alexiou C, Ohri SK, Haw MP, Livesey SA, et al. Mitral valve surgery for acute papillary muscle rupture following myocardial infarction. J Heart Valve Dis 2002;11:27-31.
50. Russo A, Suri RM, Grigioni F, Roger VL, Oh JK, Mahoney DW, et al. Clinical outcome after surgical correction of mitral regurgitation due to papillary muscle rupture. Circulation 2008;118:1528-34.
51. Hahn RT, Abraham T, Adams MS, Bruce CJ, Glas KE, Lang RM, et al. Guidelines for performing a comprehensive transesophageal echocardiographic examination: recommendations from the american society of echocardiography and the society of cardiovascular anesthesiologists. J Am Soc Echocardiogr 2013;26:921-64.
52. Biaggi P, Jedrzkiewicz S, Gruner C, Meineri M, Karski J, Vegas A, et al. Quantification of mitral valve anatomy by three-dimensional

transesophageal echocardiography in mitral valve prolapse predicts surgical anatomy and the complexity of mitral valve repair. J Am Soc Echocardiogr 2012;25:758-65.
53. Foster GP, Isselbacher EM, Rose GA, Torchiana DF, Akins CW, Picard MH. Accurate localization of mitral regurgitant defects using multiplane transesophageal echocardiography. Ann Thorac Surg 1998;65:1025-31.
54. Lambert AS, Miller JP, Merrick SH, Schiller NB, Foster E, Muhiudeen-Russell I, et al. Improved evaluation of the location and mechanism of mitral valve regurgitation with a systematic transesophageal echocardiography examination. Anesth Analg 1999;88:1205-12.
55. Maslow A, Schwartz C, Bert A. Pro: single-plane echocardiography provides an accurate and adequate examination of the native mitral valve. J Cardiothorac Vasc Anesth 2002;16:508-14.
56. Bollen BA, He Luo H, Oury JH, Rubenson DS, Savage RM, Duran CM. Case 4-2000: a systematic approach to intraoperative transesophageal echocardiographic evaluation of the mitral valve apparatus with anatomic correlation. J Cardiothorac Vasc Anesth 2000;14:330-8.
57. Mahmood F, Hess PE, Matyal R, Mackensen GB, Wang A, Qazi A, et al. Echocardiographic anatomy of the mitral valve: a critical appraisal of 2-dimensional imaging protocols with a 3-dimensional perspective. J Cardiothorac Vasc Anesth 2012;26:777-84.
58. Hien MD, Rauch H, Lichtenberg A, De Simone R, Weimer M, Ponta OA, et al. Real-time three-dimensional transesophageal echocardiography: improvements in intraoperative mitral valve imaging. Anesth Analg 2013;116:287-95.
59. Ben Zekry S, Nagueh SF, Little SH, Quinones MA, McCulloch ML, Karanbir S, et al. Comparative accuracy of two- and three-dimensional transthoracic and transesophageal echocardiography in identifying mitral valve pathology in patients undergoing mitral valve repair: initial observations. J Am Soc Echocardiogr 2011;24:1079-85.
60. Lang RM, Badano LP, Tsang W, Adams DH, Agricola E, Buck T, et al. EAE/ASE recommendations for image acquisition and display using three-dimensional echocardiography. J Am Soc Echocardiogr 2012;25:3-46.
61. Aybek T, Doss M, Abdel-Rahman U, Simon A, Miskovic A, Risteski PS, et al. Echocardiographic assessment in minimally invasive mitral valve surgery. Med Sci Monit 2005;11:27-32.
62. Wang Y, Gao CQ, Wang G, Wang JL. Transesophageal echocardiography guided cannulation for peripheral cardiopulmonary bypass during robotic cardiac surgery. Chin Med J 2012;125:3236-9.
63. Caldarera I, Van Herwerden LA, Taams MA, Bos E, Roelandt JR. Multiplane transoesophageal echocardiography and morphology of regurgitant mitral valves in surgical repair. Eur Heart J 1995;16:999-1006.
64. Shah PM, Raney AA. Echocardiography in mitral regurgitation with relevance to valve surgery. J Am Soc Echocardiogr 2011;24:1086-91.
65. Pierard LA, Carabello BA. Ischaemic mitral regurgitation: pathophysiology, outcomes and the conundrum of treatment. Eur Heart J 2010;31:2996-3005.
66. Silbiger JJ. Mechanistic insights into ischemic mitral regurgitation: echocardiographic and surgical implications. J Am Soc Echocardiogr 2011;24:707-19.
67. Lee AP, Acker M, Kubo SH, Bolling SF, Park SW, Bruce CJ, et al. Mechanisms of recurrent functional mitral regurgitation after mitral valve repair in nonischemic dilated cardiomyopathy: importance of distal anterior leaflet tethering. Circulation 2009;119:2606-14.
68. Zoghbi WA, Enriquez-Sarano M, Foster E, Grayburn PA, Kraft CD, Levine RA, et al. Recommendations for evaluation of the severity of native valvular regurgitation with two-dimensional and Doppler echocardiography. J Am Soc Echocardiogr 2003;16:777-802.
69. Lancellotti P, Moura L, Pierard LA, Agricola E, Popescu BA, Tribouilloy C, et al. European Association of Echocardiography recommendations for the assessment of valvular regurgitation. Part 2: mitral and tricuspid regurgitation (native valve disease). Eur J Echocardiogr 2010;11:307-32.
70. Vahanian A, Alfieri O, Andreotti F, Antunes MJ, Baron-Esquivias G, Baumgartner H, et al. Guidelines on the management of valvular heart disease (version 2012): the Joint Task Force on the Management of Valvular Heart Disease of the European Society of Cardiology (ESC) and the European Association for Cardio-Thoracic Surgery (EACTS). Eur Heart J 2012;33:2451-96.
71. Pu M, Prior DL, Fan X, Asher CR, Vasquez C, Griffin BP, et al. Calculation of mitral regurgitant orifice area with use of a simplified proximal convergence method: initial clinical application. J Am Soc Echocardiogr 2001;14:180-5.
72. Zeng X, Levine RA, Hua L, Morris EL, Kang Y, Flaherty M, et al. Diagnostic value of vena contracta area in the quantification of mitral regurgitation severity by color Doppler 3D echocardiography. Circ Cardiovasc Imaging 2011;4:506-13.
73. Grewal KS, Malkowski MJ, Piracha AR, Astbury JC, Kramer CM, Dianzumba S, et al. Effect of general anesthesia on the severity of mitral regurgitation by transesophageal echocardiography. Am J Cardiol 2000;85:199-203.
74. Chin JH, Lee EH, Choi DK, Choi IC. The effect of depth of anesthesia on the severity of mitral regurgitation as measured by transesophageal echocardiography. J Cardiothorac Vasc Anesth 2012;26:994-8.
75. Schwammenthal E, Chen C, Benning F, Block M, Breithardt G, Levine RA. Dynamics of mitral regurgitant flow and orifice area. Physiologic application of the proximal flow convergence method: clinical data and experimental testing. Circulation 1994;90:307-22.
76. Hung J, Otsuji Y, Handschumacher MD, Schwammenthal E, Levine RA. Mechanism of dynamic regurgitant orifice area variation in functional mitral regurgitation: physiologic insights from the proximal flow convergence technique. J Am Coll Cardiol 1999;33:538-45.
77. Grayburn PA, Weissman NJ, Zamorano JL. Quantitation of mitral regurgitation. Circulation 2012;126:2005-17.
78. Kahlert P, Plicht B, Schenk IM, Janosi RA, Erbel R, Buck T. Direct assessment of size and shape of noncircular vena contracta area in functional versus organic mitral regurgitation using real-time three-dimensional echocardiography. J Am Soc Echocardiogr 2008;21:912-21.
79. Marsan NA, Westenberg JJ, Ypenburg C, Delgado V, van Bommel RJ, Roes SD, et al. Quantification of functional mitral regurgitation by real-time 3D echocardiography: comparison with 3D velocity-encoded cardiac magnetic resonance. JACC Cardiovasc Imaging 2009;2:1245-52.
80. Lancellotti P, Troisfontaines P, Toussaint AC, Pierard LA. Prognostic importance of exercise-induced changes in mitral regurgitation in patients with chronic ischemic left ventricular dysfunction. Circulation 2003;108:1713-7.
81. Adams DH, Rosenhek R, Falk V. Degenerative mitral valve regurgitation: best practice revolution. Eur Heart J 2010;31:1958-66.
82. Verma S, Mesana TG. Mitral-valve repair for mitral-valve prolapse. N Engl J Med 2009;361:2261-9.
83. Perier P, Hohenberger W, Lakew F, Batz G, Urbanski P, Zacher M, et al. Toward a new paradigm for the reconstruction of posterior leaflet prolapse: midterm results of the "respect rather than resect" approach. Ann Thorac Surg 2008;86:718-25.
84. Meyer MA, von Segesser LK, Hurni M, Stumpe F, Eisa K, Ruchat P. Long-term outcome after mitral valve repair: a risk factor analysis. Eur J Cardiothorac Surg 2007;32:301-7.
85. Suri RM, Schaff HV, Dearani JA, Sundt TM III, Daly RC, Mullany CJ, et al. Survival advantage and improved durability of mitral repair for leaflet prolapse subsets in the current era. Ann Thorac Surg 2006;82:819-26.
86. Aubert S, Acar C. Gaping cleft or commissure–an under-rated cause of residual mitral insufficiency following valve repair: case reports. J Heart Valve Dis 2009;18:290-1.
87. Riegel AK, Busch R, Segal S, Fox JA, Eltzschig HK, Shernan SK. Evaluation of transmitral pressure gradients in the intraoperative echocardiographic diagnosis of mitral stenosis after mitral valve repair. PLoS One 2011;6:e26559.
88. Ibrahim M, Rao C, Ashrafian H, Chaudhry U, Darzi A, Athanasiou T. Modern management of systolic anterior motion of the mitral valve. Eur J Cardiothorac Surg 2012;41:1260-70.
89. He S, Hopmeyer J, Lefebvre XP, Schwammenthal E, Yoganathan AP, Levine RA. Importance of leaflet elongation in causing systolic anterior motion of the mitral valve. J Heart Valve Dis 1997;6:149-59.

90. Shah PM, Raney AA. Echocardiographic correlates of left ventricular outflow obstruction and systolic anterior motion following mitral valve repair. J Heart Valve Dis 2001;10:302-6.
91. Lee KS, Stewart WJ, Savage RM, Loop FD, Cosgrove DM III. Systolic anterior motion of mitral valve after the posterior leaflet sliding advancement procedure. Ann Thorac Surg 1994;57:1338-40.
92. Maslow AD, Regan MM, Haering JM, Johnson RG, Levine RA. Echocardiographic predictors of left ventricular outflow tract obstruction and systolic anterior motion of the mitral valve after mitral valve reconstruction for myxomatous valve disease. J Am Coll Cardiol 1999;34:2096-104.
93. Quigley RL. Prevention of systolic anterior motion after repair of the severely myxomatous mitral valve with an anterior leaflet valvuloplasty. Ann Thorac Surg 2005;80:179-82.
94. Raney AA, Shah PM, Joyo CI. The "Pomeroy procedure": a new method to correct post-mitral valve repair systolic anterior motion. J Heart Valve Dis 2001;10:307-11.
95. Perier P, Clausnizer B, Mistarz K. Carpentier "sliding leaflet" technique for repair of the mitral valve: early results. Ann Thorac Surg 1994;57:383-6.
96. Varghese R, Anyanwu AC, Itagaki S, Milla F, Castillo J, Adams DH. Management of systolic anterior motion after mitral valve repair: an algorithm. J Thorac Cardiovasc Surg 2012;143:S2-7.
97. Crescenzi G, Landoni G, Zangrillo A, Guarracino F, Rosica C, La Canna G, et al. Management and decision-making strategy for systolic anterior motion after mitral valve repair. J Thorac Cardiovasc Surg 2009;137:320-5.
98. Grande AM, Fiore A, Massetti M, Vigano M. Iatrogenic circumflex coronary lesion in mitral valve surgery: case report and review of the literature. Tex Heart Inst J 2008;35:179-83.